Universiteit Utrecht

Master's Thesis

Institute of Theoretical Physics

Dynamical eigenmodes of various bead-spring systems

arXiv:1210.0774 **[cond-mat.soft]** arXiv:1212.1024 **[cond-mat.soft]**

R. Keesman

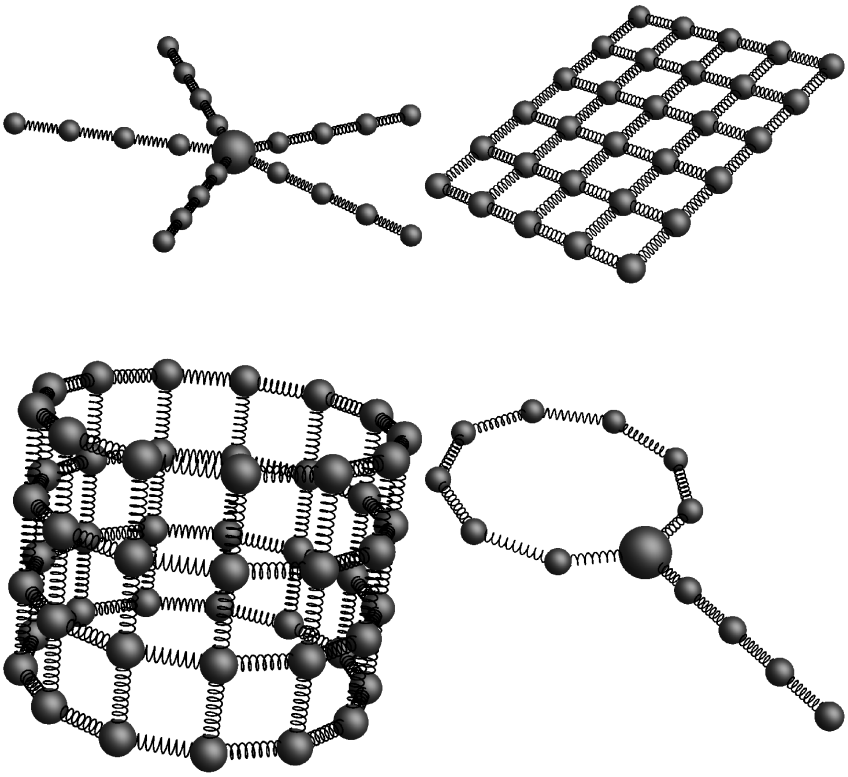

February 21, 2013

Supervisor:
Prof. dr. G. T. Barkema
Institute of Theoretical Physics
University of Utrecht
Co-supervisor:
dr. D. Panja

Abstract

We study the dynamics of polymers using the bead-spring model in the overdamped limit. In particular we take a look at phantom bead-spring chains with the topology of symmetric stars, tadpoles and polymerized phantom manifolds. After briefly reviewing how the bead-spring model has been applied to study the dynamics of linear polymers, we apply similar methods to solve the equations of motion for bead-spring systems of more complex topologies using the so-called Rouse modes. These eigenmodes allow full analytical calculations of virtually any static or dynamical quantity. As examples we determine radii of gyration, mean square displacements of tagged monomers, and autocorrelation functions of vectors that span between two tagged monomers. Interestingly, even in the presence of tensile forces of any magnitude the Rouse modes remain the exact eigenmodes for the membrane, a two-dimensional manifold. With stronger forces the membrane becomes essentially flat, and does not get the opportunity to intersect itself; in such a situation our analysis provides a useful and exactly soluble approach to the dynamics for a realistic model flat membrane under tension. Parts of these results are accepted for publication[1, 2].

Contents

1 Introduction

Bead-spring models play a central role in the theory and modeling of polymer dynamics. Most of the applications of bead-spring models (and polymer dynamics in general) are for linear polymers, for which the polymer consists of a linear sequence of beads connected by harmonic springs. The reason why, to date, the Rouse model deserves a special mention, lies in the fact that it allows full analytical calculations of virtually any dynamical quantity. Rather than the equations of motion for the individual beads, one considers the so-called Rouse modes.

Using the definition of Rouse modes it has been shown in recent works that the dynamics of a tagged bead in a linear bead-spring model is described by the Generalized Langevin Equation (GLE) [6, 7], and that the dynamics of polymers with steric repulsion (also known as self-avoiding polymer chains) [8], as well as of those in melts as described by the repton model [9] can be well-approximated. Here, we continue this line of research, but now we are interested in exact solutions of the dynamical properties of polymers with the topology of stars and manifolds.

In Sec. 2 we explain the bead-spring model that provides the framework for all the research on various types of polymers that follows. In Sec. 3 this model is applied to linear polymers, which is well established work. It contains a detailed proof for the solutions of the equations of motion and how it can be used to obtain information about the behavior of such a polymer. We then apply the bead-spring model to star polymers in Sec. 4, tadpole polymers in Sec. 5, and polymerized membranes in Sec. 6 and present some statical and dynamical quantities of interest for these various types of polymers. We end the thesis with a discussion in Sec. 7.

2 Bead-spring model

2.1 Brownian motion

A fluid containing a single polymer molecule will have too many degrees of freedom to describe classically because of the sheer number of particles that the fluid consists of. Instead we only consider the degrees of freedom in the polymer whilst describing the fluid stochastically.

We start off with a single spherical particle (bead) in a three-dimensional fluid where its size is significantly larger than that of the particles that make up the fluid. In a very short amount of time the bead will collide with many of the fluid particles resulting in some random thermal force $\mathbf{g}$. Even though we do not know the specifics of the forces from the fluid acting on the bead, the central limit theorem states that we can assume the resulting force to follow a Gaussian distribution. To ensure that the probability distribution function of the position of the bead is equal to the Boltzmann distribution, the thermal forces will have the properties

$$\langle \mathbf{g}(t) \rangle = \mathbf{0}, \tag{1a}$$

$$\langle \mathbf{g}(t) \cdot \mathbf{g}(t') \rangle = \frac{6k_B T}{\zeta} \delta(t - t'), \tag{1b}$$

with Boltzmann constant k_B and temperature T. We approximate the variance as completely uncorrelated in time since the dynamics of the bead has a much larger time scale than that of the particles in the fluid. In general the bead in the fluid will also have some viscous friction constant ζ that slows down the bead moving in the solvent. The equations of motion for such a bead with mass m and position $\mathbf{R}(t)$ in a potential field become

$$m \frac{d^2 \mathbf{R}}{dt^2} = -\zeta \frac{d\mathbf{R}}{dt} - \frac{\partial U}{\partial \mathbf{R}} + \zeta \mathbf{g}, \tag{2}$$

with U the potential energy of the system. For a highly viscous fluid the system will be overdamped, meaning that the inertial terms are negligible. Since this is typically the case for polymeric systems, we can use the Langevin equation

$$\frac{d\mathbf{R}}{dt} = -\frac{1}{\zeta} \frac{\partial U}{\partial \mathbf{R}} + \mathbf{g}. \tag{3}$$

2.2 Rouse theory

To investigate the behavior of a polymer we use the so-called bead-spring model. We connect the beads by ideal springs of length zero. For the position of the beads $\mathbf{R}_n(t)$ the equations of motion are then given by

$$\frac{d\mathbf{R}_n}{dt} = -\frac{1}{\zeta} \frac{\partial U}{\partial \mathbf{R}_n} + \mathbf{g}_n, \tag{4}$$

with potential energy

$$U = \frac{k}{2} \sum_{<m,n>} (\mathbf{R}_m - \mathbf{R}_n)^2, \tag{5}$$

where the sum is over all pairs of beads connected by a spring. In addition, the thermal forces are not only uncorrelated in time but also between different beads so that $\langle \mathbf{g}_m(t) \cdot \mathbf{g}_n(t') \rangle = (6k_B T/\zeta)\delta_{mn}\delta(t - t')$.

3 Linear polymer

The bead-spring model from the previous section creates a framework to theoretically study any type of polymer. It has been successfully applied to linear polymers[4, 5] for which the dynamics of the polymer could be solved in the long polymer limit. In this section we show how the equations of motion can be solved exactly by means of eigenmodes and how they can be used to calculate the mean square displacement of the monomer in the middle of the polymer, as an example. As an extension we also provide the eigenmodes for a linear polymer with the ends tied together into a ring polymer.

3.1 Eigenmodes

Linear polymers consisting of $N+1$ identical segments can be made in the bead-spring model by connecting each of the identical beads, except those at the end, to two other beads and thus creating a linear chain. Internally labeling the beads $n = 0 \dots N$ results in an explicit form of the potential energy

$$U = \frac{k}{2} \sum_{n=1}^{N} \left(\mathbf{R}_n - \mathbf{R}_{n-1} \right)^2 . \tag{6}$$

If we define $\mathbf{R}_{-1} \equiv \mathbf{R}_0$ and $\mathbf{R}_{N+1} \equiv \mathbf{R}_N$ the equations of motion become

$$\frac{d\mathbf{R}_n}{dt} = -\frac{k}{\zeta} \left(2\mathbf{R}_n - \mathbf{R}_{n+1} - \mathbf{R}_{n-1} \right) + \mathbf{g}_n. \tag{7}$$

This model was first proposed by P.E. Rouse, and so is called the Rouse model[3].

The set of differential equations from Eq. (7) is coupled but can be solved by making a transformation from positions of the beads to so-called eigenmodes for which the differential equations are simply linear. Note that all of the following calculations and solutions in terms of eigenmodes are still valid even in case of the general Langevin equation (2) where the inertial term is still included since the trouble is here linearizing the right hand side of the differential equations. After solving the equations of motion for the eigenmodes, many quantities of interest can be expressed in terms of these solutions and thus they provide valuable and analytical insight in the behavior of the polymer. We start by defining the eigenmodes in terms of the positions of the beads and the inverse as

$$\mathbf{X}_p(t) = \frac{1}{N+1} \sum_{n=0}^{N} \cos \left[\frac{\pi (n+1/2) p}{N+1} \right] \mathbf{R}_n(t), \tag{8}$$

$$\mathbf{R}_n = \mathbf{X}_0 + 2 \sum_{p=1}^{N} \cos \left[\frac{\pi (n+1/2) p}{N+1} \right] \mathbf{X}_p. \tag{9}$$

Note that the zeroth eigenmode is the position of the center of mass, given that all beads are identical. This transformation is also known as the discrete cosine transform and reversibility is easily shown by using the orthogonality relation for which the proof can be found in Appendix B.

By taking the time derivative in Eq. (8) and filling in Eq. (7) we get a set of time derivatives of the eigenmodes equal to some sum over positions of all the beads. We use the inverse in Eq. (9) such that the set of differential equations is solely expressed in terms of the eigenmodes, which yields

$$\begin{aligned} \frac{d\mathbf{X}_p}{dt} =& \frac{1}{N+1} \sum_{n=0}^{N} \cos \left[\frac{\pi (n+1/2) p}{N+1} \right] \mathbf{g}_n - \frac{2}{N+1} \frac{k}{\zeta} \sum_{n=0}^{N} \sum_{q=1}^{N} \cos \left[\frac{\pi (n+1/2) p}{N+1} \right] \times \\ & \left\{ 2 \cos \left[\frac{\pi (n+1/2) q}{N+1} \right] - \cos \left[\frac{\pi (n+3/2) q}{N+1} \right] - \cos \left[\frac{\pi (n-1/2) q}{N+1} \right] \right\} \mathbf{X}_q. \end{aligned} \tag{10}$$

The first term, which we will denote as $\mathbf{G}_p$, is the transform of thermal force $\mathbf{g}_n$ and the second term can be simplified by using trigonometric identities, namely the angle sum and difference identities and the power-reduction formula, so that this can be rewritten as

$$\frac{d\mathbf{X}_p}{dt} = \mathbf{G}_p - \frac{8}{N+1} \frac{k}{\zeta} \sum_{n=0}^{N} \sum_{q=1}^{N} \cos \left[\frac{\pi (n+1/2) p}{N+1} \right] \cos \left[\frac{\pi (n+1/2) q}{N+1} \right] \sin^2 \left[\frac{\pi q/2}{N+1} \right] \mathbf{X}_q. \tag{11}$$

Using Eq. (102a) the equations of motion for the eigenmodes are reduced to

$$\frac{d\mathbf{X}_p}{dt} = \begin{cases} -\alpha_p \mathbf{X}_p + \mathbf{G}_p & , p = 1 \dots N \\ \mathbf{G}_0 & , p = 0 \end{cases} \tag{12a}$$

$$\text{with } \alpha_p \equiv 4\frac{k}{\zeta}\sin^2\left[\frac{\pi p/2}{N+1}\right]. \tag{12b}$$

Because of the thermal forces these differential equations can only be solved in terms of the time-averaged values of the eigenmodes. Because the thermal forces are zero on average the time-averaged value of the eigenmodes will also be zero. A much more interesting quantity is the variance of the amplitudes of the modes. To do this we must first look at the correlation functions of the various transformations of the thermal forces $\mathbf{G}_p$. The correlation functions for the thermal forces can be used in combination with the orthogonality relation from Eq. (102a) to calculate the correlation functions for the transform $\mathbf{G}_p$. The only non-vanishing correlation functions are

$$\langle \mathbf{G}_0(t) \cdot \mathbf{G}_0(t') \rangle = \frac{6k_BT}{\zeta(N+1)}\delta(t-t'), \tag{13a}$$

$$\langle \mathbf{G}_p(t) \cdot \mathbf{G}_q(t') \rangle = \frac{3k_BT}{\zeta(N+1)}\delta_{pq}\delta(t-t'). \tag{13b}$$

With Eqs. (13) the mode amplitude correlation functions can be calculated as shown in Appendix C. While all cross correlation functions are zero we find that

$$X_{00}(t) \equiv \langle [\mathbf{X}_0(t) - \mathbf{X}_0(0)]^2 \rangle \equiv \langle [\mathbf{R}_{\rm cm}(t) - \mathbf{R}_{\rm cm}(0)]^2 \rangle = \frac{6k_BT}{\zeta(N+1)}t, \tag{14a}$$

$$X_{pq}(t) \equiv \langle \mathbf{X}_p(t) \cdot \mathbf{X}_q(0) \rangle = \frac{3k_BT}{\zeta(N+1)}\frac{1}{2\alpha_p}\exp\left[-\alpha_p t\right]\delta_{pq}. \tag{14b}$$

As the zeroth eigenmode equals the position of the center of mass, we note that the polymer as a whole has the same diffusive behavior as a single bead but with friction coefficient $N+1$ times as large whereas the correlation for a mode at different times decay exponentially. This set of eigenmode amplitude correlation functions can be used to analytically calculate virtually any quantity of interest for the polymer.

3.2 Mean square displacement of the central bead

As an example we use the eigenmode amplitude correlation functions to investigate the mean square displacement of a monomer in the middle of a linear polymer. We start by defining

$$\Delta\mathbf{R}_{\rm m}(t) \equiv \mathbf{R}_{N/2}(t) - \mathbf{R}_{N/2}(0), \tag{15}$$

which can be rewritten as

$$\Delta\mathbf{R}_{\rm m}(t) = \mathbf{X}_0(t) - \mathbf{X}_0(0) + 2\sum_{p=1}^{N}\cos\left[\frac{\pi p}{2}\right]\left\{\mathbf{X}_p(t) - \mathbf{X}_p(0)\right\}. \tag{16}$$

The mean square displacement of a monomer in the middle of a linear polymer is given by

$$\langle \Delta\mathbf{R}_{\rm m}^2(t) \rangle = \langle [\mathbf{R}_{cm}(t) - \mathbf{R}_{cm}(0)]^2 \rangle + 8\sum_{p,q=1}^{N,N}\cos\left[\frac{\pi p}{2}\right]\cos\left[\frac{\pi q}{2}\right]\left\{X_{pq}(0) - X_{pq}(t)\right\} \tag{17}$$

$$\langle \Delta\mathbf{R}_{\rm m}^2(t) \rangle = \frac{6k_BT}{\zeta(N+1)}t + \frac{12k_BT}{\zeta(N+1)}\sum_{p\in\text{ even}}\frac{1}{\alpha_p}\left\{1 - \exp\left[-\alpha_p t\right]\right\}, \tag{18}$$

where Eq. (14) was used. On very short time scales $kt/\zeta < 1/4$ the exponent can be expanded up to first order so that the summation becomes p-independent. The mean square displacement then becomes exactly $\langle \Delta\mathbf{R}_{\rm m}^2(t) \rangle = (6k_BT/\zeta)t$ which is the mean square displacement for a single free bead. For moderate time values the sum can be converted to an integral in the long polymer limit. For very long times $kt/\zeta \gg N^2/3$ the sum is capped and the mean square displacement of the center of mass will

dominate.

$$\langle \Delta \mathbf{R}_{\mathrm{m}}^2(t) \rangle = \frac{6k_BT}{\zeta(N+1)} t + 6\frac{k_BT}{\pi^2 k} N \int_0^\infty \frac{dx}{x^2} \left\{ 1 - \exp\left[-\frac{k\pi^2}{\zeta} \frac{t}{N^2} x^2 \right] \right\}, \tag{19}$$

$$\langle \Delta \mathbf{R}_{\mathrm{m}}^2(t) \rangle = \frac{6k_BT}{\zeta(N+1)} t + 6k_BT \sqrt{\frac{t}{\pi k \zeta}}. \tag{20}$$

So we find that for very early times the mean square displacement of a monomer in the middle of a polymer will be equal to that of a single free bead. After some time has passed the monomer will feel the connectivity to the rest of the polymer and so the movement is restricted. At very large times this connectivity is negligible compared to the mean square displacement of the whole polymer and so it will act like a single bead with a friction coefficient $N+1$ as large as for the single bead.

3.3 Ring polymer

When a linear polymer has its ends connected it becomes a ring polymer which has a very similar behavior. Although in itself this does not add very much to the knowledge on polymers, we do however use the eigenmodes for the ring polymers to extend the range of polymers for which we can solve the equations of motion. The eigenmodes for the ring polymer allow for periodic boundary conditions in the star polymer, of which the tadpole is an example, and in the polymerized membrane. Consider a ring polymer with $N+1$ beads internally labeled $n = 0 \ldots N$. The eigenmodes are then given by

$$\mathbf{C}_p(t) = \frac{1}{N+1} \sum_{n=0}^{N} \cos\left[\frac{2\pi(n+1/2)p}{N+1} \right] \mathbf{R}_n(t), \qquad p = 0 \ldots \lfloor N/2 \rfloor, \tag{21a}$$

$$\mathbf{S}_p(t) = \frac{1}{N+1} \sum_{n=0}^{N} \sin\left[\frac{2\pi(n+1/2)p}{N+1} \right] \mathbf{R}_n(t), \qquad p = 1 \ldots \lceil N/2 \rceil, \tag{21b}$$

where $\lceil x \rceil$ and $\lfloor x \rfloor$ are the ceiling and floor function respectively.

4 Star polymer

Besides the heavily studied linear polymer chains there are many other types of polymers whose dynamics deserve closer inspection. In this section we concern ourselves with the dynamics of bead-spring chains that have the topology of a symmetric star (with f arms). We present the dynamical eigenmodes, and use the mode amplitudes to provide analytical expressions for the radius of gyration, mean square displacement of a tagged monomer, and the autocorrelation function of the vector that spans from the center of the star to a bead on one of the arms.

4.1 Eigenmodes

A major difficulty for dynamics of polymers with a more complex topology like the symmetric star polymer is that in most cases an elegant analytical expression for the set of dynamical eigenmodes cannot be found [10]. Here we show that for a symmetric star polymer with a special central bead the dynamical eigenmodes can indeed be written down exactly, and subsequently the dynamical behavior of many interesting physical quantities can be determined precisely. For simplicity, in commensuration with the Rouse model, henceforth we term these dynamical eigenmodes as Rouse modes. Specifically, we consider a star polymer with f identical arms, each consisting of N identical beads, connected to a central bead whose hydrodynamic radius is f times as big as the other ones, i.e., its viscous drag is f times as large. A graphical representation of such a star polymer with $f = 5$ and $N = 4$ can be found in Fig. 1. It is worthwhile to note in this context that a key method to synthesize a star polymer chain is to attach the arms, which are linear chains, to a multivalent central core with sticky ends (see, e.g., Ref. [11] and the references cited therein). Although from the synthesis process it is realistic that the core has a significantly higher hydrodynamic radius, the choice in our simplified model to make hydrodynamic radius of the central bead exactly f times as the other beads is motivated by our strive to determine the Rouse modes exactly. For modestly-sized chains, where the hydrodynamic radius of the core is not f times as big as the arm beads, the dynamical matrix (the homogenous part of the dynamical differential equation) has been diagonalized numerically, yielding the numerical identification of the Rouse modes [10].

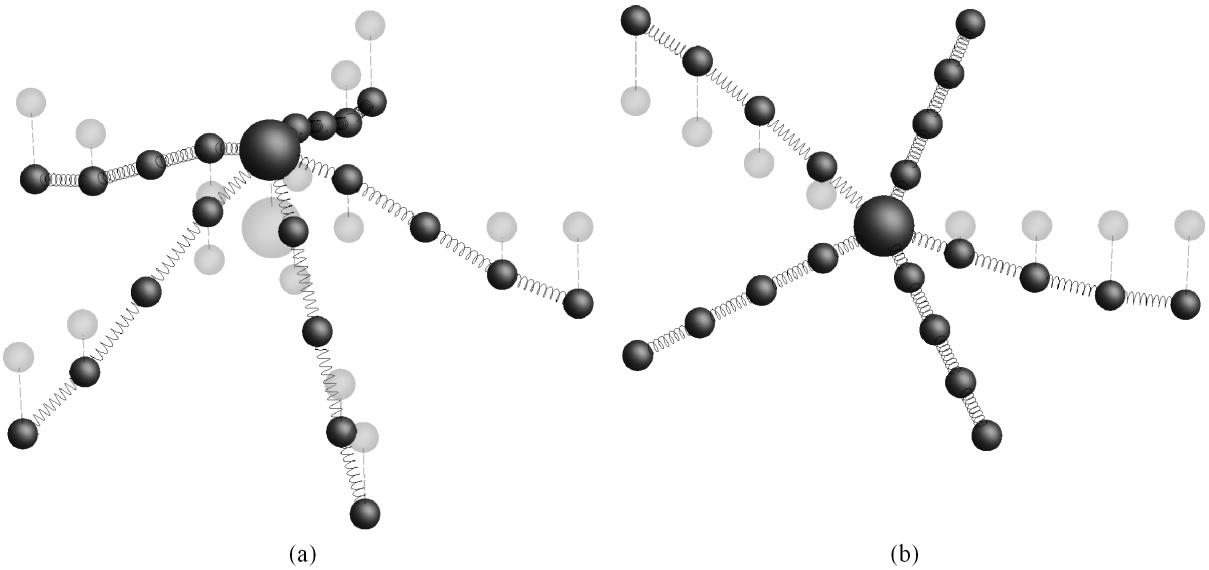

Figure 1: Two graphical representations of a symmetrical star polymer to visualize the Rouse modes. Depicted is a symmetric starpolymer with five arms consisting of four beads each and a central monomer which has a friction coefficient five times that of beads in the arms. The transparent configurations are polymers in the origin stretched in the xy-plane for visual convenience with no Rouse mode excited in the z-direction. The opaque configurations are like the transparent ones but with a pure $\mathbf{X}_1$ mode (a) and $\mathbf{Y}_1^{(i,j)}$ modes (b) in the z-direction.

We label the position of the central bead as $\mathbf{R}_0$ and let $\mathbf{R}_{a,n}$ be the position of the n-th bead,

$n = 1 \dots N$, in the a-th arm, $a = 1 \dots f$. We consider two types of Rouse modes given by

$$\mathbf{X}_p(t) = \frac{1}{N+1}\left\{\cos\left[\frac{\pi p/2}{N+1}\right]\mathbf{R}_0(t) + \frac{1}{f}\sum_{a,n=1}^{f,N}\cos\left[\frac{\pi(n+1/2)p}{N+1}\right]\mathbf{R}_{a,n}(t)\right\}, \tag{22a}$$

$$\mathbf{Y}_q^{(i,j)}(t) = \frac{1}{2N+1}\sum_{n=1}^{N}\cos\left[\frac{\pi(N-n+1/2)(q-1/2)}{N+1/2}\right](\mathbf{R}_{i,n}(t) - \mathbf{R}_{j,n}(t)), \tag{22b}$$

with $p = 0 \dots N$ and $q = 1 \dots N$. A visualization of the two kinds of modes can also be found in Fig. 1. The first set of modes $\mathbf{X}_p(t)$ are like Rouse modes for a linear polymer through all the arms. The second set of modes $\mathbf{Y}_p^{(i,j)}(t)$ can also be thought of as Rouse modes as in Eq. (8) with p odd valued and through a linear chain of length $2N+1$ made up by arms i and j and the central bead. There are $Nf(f-1)/2$ modes of the type $\mathbf{Y}_p^{(i,j)}(t)$ with $i < j$, but the total set of these modes contain only $(f-1)N$ independent degrees of freedom, for instance because $\mathbf{Y}_p^{(i,k)}(t) = \mathbf{Y}_p^{(i,j)}(t) + \mathbf{Y}_p^{(j,k)}(t)$; we could have constructed, for every p, an orthogonal set of $f-1$ modes out of the full set of modes $\mathbf{Y}_p^{(i,j)}(t)$, but we choose not to do that for the sake of mathematical elegance. Combined with $N+1$ modes $\mathbf{X}_p(t)$, the total set contains $fN+1$ three-dimensional modes needed to describe the system that has $fN+1$ beads so that the number of degrees of freedom is the same.

In similar fashion as for the linear polymer the equations of motion for the eigenmodes can be written down and the correlation function for the amplitudes of the eigenmodes solved. We define

$$\alpha_{\mathbf{Y}_p} \equiv 4\frac{k}{\zeta}\sin^2\left[\frac{\pi(p-1/2)}{2N+1}\right], \tag{23a}$$

$$\alpha_{\mathbf{X}_p} = 4\frac{k}{\zeta}\sin^2\left[\frac{\pi p}{2N+2}\right], \tag{23b}$$

so that the dynamics of these modes for a star polymer are captured by

$$\langle[\mathbf{X}_0(t) - \mathbf{X}_0(0)]^2\rangle = \frac{6k_BT}{\zeta f(N+1)}t \tag{24a}$$

$$\langle\mathbf{X}_p(t)\cdot\mathbf{X}_q(0)\rangle = \frac{3k_BT}{\zeta f(N+1)}\frac{1}{2\alpha_{\mathbf{X}_p}}\exp\left[-\alpha_{\mathbf{X}_p}t\right]\delta_{pq} \tag{24b}$$

$$\langle\mathbf{Y}_p^{(i,j)}(t)\cdot\mathbf{Y}_q^{(k,l)}(0)\rangle = \frac{3k_BT}{\zeta(2N+1)}\frac{\delta_{(i,j)(k,l)}}{2}\frac{1}{2\alpha_{\mathbf{Y}_p}}\exp\left[-\alpha_{\mathbf{Y}_p}t\right]\delta_{pq}, \tag{24c}$$

where $\delta_{(i,j)(k,l)} = \delta_{ik} - \delta_{jk} - \delta_{il} + \delta_{jl}$. This is supplemented by $X_{00}(t) \equiv \langle[\mathbf{X}_0(t) - \mathbf{X}_0(0)]^2\rangle = 6k_BTt/(\zeta f(N+1))$ and all other correlations between modes strictly zero. The derivations of the Rouse mode amplitudes can be found in Appendix D.

4.2 Radius of gyration

The squared radius of gyration is defined as the weighted sum over all differences between the position of a monomer and the center of mass squared. Below we work out the radius of gyration for the case of the star polymer where the central monomer is f times heavier than the other beads, although the radius of gyration can be calculated following the same line for other cases as well. In the former case the location of the center-of-mass $\mathbf{R}_{\rm cm}(t) \equiv \mathbf{X}_0(t)$, and the squared radius of gyration is defined as

$$R_g^2 = \frac{1}{f(N+1)}\left[f\langle[\mathbf{R}_0(t) - \mathbf{R}_{\rm cm}(t)]^2\rangle + \sum_{i,n=1}^{f,N}\langle[\mathbf{R}_{i,n}(t) - \mathbf{R}_{\rm cm}(t)]^2\rangle\right], \tag{25}$$

which can be calculated by plugging in Eq. (117). This reduces to

$$R_g^2 = 2\sum_{p=1}^{N}X_{pp}(0) + \frac{4(2N+1)}{f^3(N+1)}\sum_{p,i,j,k=1}^{N,f,f,f}Y_{pp}^{(i,j)(i,k)}(0). \tag{26}$$

Plugging in Eq. (24) explicitly and taking the long polymer limit yields

$$R_g^2 = \frac{3k_BT}{k\pi^2}\frac{N}{f}\sum_{p=1}^{\infty}\frac{1}{p^2} + \frac{3k_BT}{k\pi^2}\frac{N}{f^3}\sum_{i,j,k=1}^{f,f,f}\delta_{(i,j)(i,k)}\sum_{p=1}^{\infty}\frac{1}{(p-1/2)^2}. \tag{27}$$

The sums can be evaluated by using Eq. (106).

And so the radius of gyration squared for a long symmetric star polymer becomes

$$R_g^2 = \frac{k_B T N}{k} \frac{3f-2}{2f}. \tag{28}$$

This result is consistent with that of a linear chain ($f = 1$).

4.3 Mean square displacement of a bead

We now consider the mean square displacement of the central bead and a bead in an arm for a star polymer with long arms. We start by defining the displacement vector for the central bead and writing it in terms of modes using Eq. (117a):

$$\begin{aligned}\Delta\mathbf{R}_0(t) \equiv& \mathbf{R}_0(t) - \mathbf{R}_0(0) \\ =& \mathbf{X}_0(t) - \mathbf{X}_0(0) + 2\sum_{p=1}^{N} \cos\left[\frac{\pi p/2}{N+1}\right] \{\mathbf{X}_p(t) - \mathbf{X}_p(0)\}.\end{aligned} \tag{29}$$

The mean square displacement is then given by

$$\langle \Delta\mathbf{R}_0^2(t)\rangle = X_{00}(t) + 8\sum_{p=1}^{N} \cos^2\left[\frac{\pi p/2}{N+1}\right] \{X_{pp}(0) - X_{pp}(t)\}, \tag{30}$$

where Eq. (24) can be plugged in, and the orthogonality of the modes was already used for simplification. Before doing so, let us look at very short time scales $kt/\zeta < 1/4$. The exponent in $X_{pq}(t)$ can then be expanded and the sum exactly evaluated using Eq. (103a), resulting in $\langle \Delta\mathbf{R}_0^2(t)\rangle = 6k_BTt/(\zeta f)$ dominating over the mean square displacement of the whole polymer which at short time scales is negligible. At very long time scales $X_{pq}(t)$ goes to zero and the term with the summation in Eq. (30) can again be exactly evaluated using Eq. (104a). So for $kt/\zeta < N^2/3$ the summation has a larger contribution than the mean square displacement of the whole polymer. For intermediate times the summation dominates and can be rewritten as an integral for very long polymers:

$$\langle \Delta\mathbf{R}_0^2(t)\rangle = \frac{12k_BT}{\pi^2 kf} \int_0^\infty \frac{dx}{x^2} \left\{1 - \exp\left[-\frac{k\pi^2 t}{\zeta} x^2\right]\right\} = \frac{12k_BT}{f}\sqrt{\frac{t}{\pi k\zeta}}. \tag{31}$$

The mean square displacement as approximated for intermediate times is greater than that of the approximation for the short time scales for $t > 4\zeta/(\pi k)$, so that is when the intermediate time regime begins. For the central bead in a star polymer the mean square displacement then becomes

$$\langle \Delta\mathbf{R}_0^2(t)\rangle = \begin{cases} \dfrac{6k_BT}{\zeta f}t, & \text{for } t < \dfrac{\zeta}{4k} \\ \dfrac{12k_BT}{f}\sqrt{\dfrac{t}{\pi k\zeta}}, & \text{for } \dfrac{4\zeta}{\pi k} < t < \dfrac{N^2\zeta}{3k} \\ \dfrac{6k_BT}{\zeta f(N+1)}t, & \text{for } t > \dfrac{N^2\zeta}{3k} \end{cases}. \tag{32}$$

Figure 2 shows the exact evaluation of Eq. (30) for some star polymer together with approximations made for the short, intermediate and long time scales found in Eq. (32). The central bead first behaves like a single bead with friction coefficient ζf. After that the movement is restricted by local connections to surrounding beads in the polymer. For very long times the position of the bead within the polymer is negligible and the mean square displacement behaves as that of a single bead with friction coefficient $\zeta f(N+1)$.

A very similar approach can be used for the mean square displacement of a bead in an arm of the star polymer, defined as

$$\begin{aligned}\Delta\mathbf{R}_n(t) \equiv& \mathbf{R}_{i,n}(t) - \mathbf{R}_{i,n}(0) \\ =& \mathbf{X}_0(t) - \mathbf{X}_0(0) + 2\sum_{p=1}^{N} \cos\left[\frac{\pi(n+1/2)p}{N+1}\right] \{\mathbf{X}_p(t) - \mathbf{X}_p(0)\} \\ &+ \frac{4}{f}\sum_{j,p=1}^{f,N} \cos\left[\frac{\pi(N-n+1/2)(p-1/2)}{N+1/2}\right] \{\mathbf{Y}_p^{(i,j)}(t) - \mathbf{Y}_p^{(i,j)}(0)\}.\end{aligned} \tag{33}$$

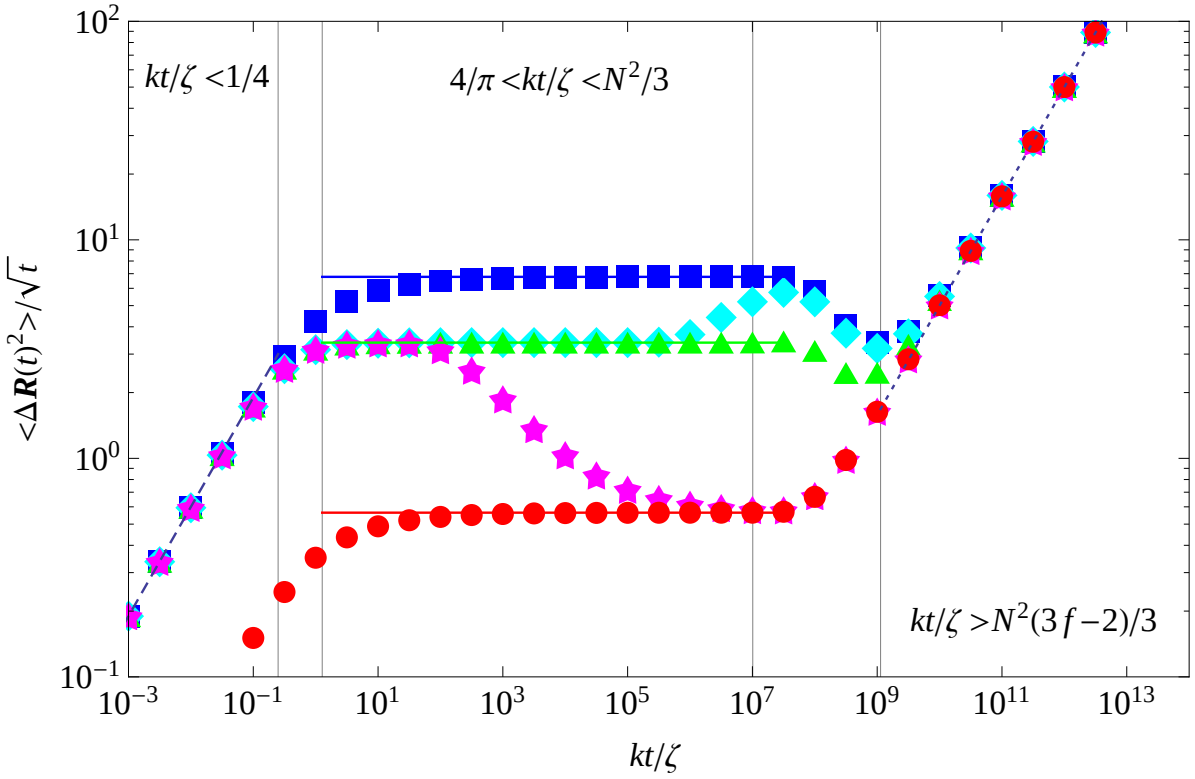

Figure 2: The scaled mean square displacement $\langle \Delta \mathbf{R}^2(t) \rangle / \sqrt{t}$ as a function of time. The mean square displacement of several beads in a symmetric star polymer as given by Eqs. (30,34) were exactly evaluated with $f = 12$ and $N = 10^4$ and other parameters put to 1. The red disks corresponds to the mean square displacement of the central bead whereas the magenta stars, green triangles, cyan diamonds, and blue squares correspond to $n = 10^{-3}N, N/2, 9N/10$, and N in Eq. (34) respectively. A bead positioned somewhere along the arm will at first behave as if it were in the middle of the arm. After time grows either the end or the center will become an influence at first and the bead will start mimicking a bead at one of those places. The short time scale $t < \zeta/(4k)$ and the very long time scale $t \gg N^2\zeta(3f-2)/(3k)$ for which $\langle \Delta \mathbf{R}^2(t) \rangle \sim t$ corresponding to the dashed and dotted lines are separated by a time during which $\langle \Delta \mathbf{R}^2(t) \rangle \sim \sqrt{t}$ corresponding to the solid lines as in agreement with Eqs. (32,36-37).

Using orthogonality of mode $\mathbf{Y}_p^{(i,j)}$ with $\mathbf{X}_q$ and with $\mathbf{Y}_q^{(k,l)}$ with $q \neq p$, and evaluating the double sum over the arms, the mean square displacement becomes

$$\begin{aligned}\langle \Delta \mathbf{R}_n^2(t) \rangle =& X_{00}(t) + 8 \sum_{p=1}^{N} \cos^2 \left[\frac{\pi(n+1/2)p}{N+1} \right] \{X_{pp}(0) - X_{pp}(t)\} \\ &+ \frac{16(f-1)}{f} \sum_{p=1}^{N} \cos^2 \left[\frac{\pi(N-n+1/2)(p-1/2)}{N+1/2} \right] \\ &\times \left\{ Y_{pp}^{(1,2)(1,2)}(0) - Y_{pp}^{(1,2)(1,2)}(t) \right\}. \end{aligned} \tag{34}$$

For small values of t the exponents can again be expanded and the sum exactly evaluated using Eqs. (103a-103b) so that in the long polymer limit $\langle \Delta \mathbf{R}_n^2(t) \rangle = 6k_BTt/\zeta$. The summation reaches its maximum, using Eqs. (104a-104b), on long time scales so that for a bead at the end of an arm the mean square displacement term of the whole polymer will start to dominate for $t > N^2\zeta(3f-2)/(3k)$. The closer a bead is to the central bead the faster its mean square displacement will behave like that of the whole polymer. We can again approximate the summation by an integral for intermediate times but

depending on the position of the bead in an arm it will behave differently.

$$\begin{aligned}\langle \Delta \mathbf{R}_n^2(t)\rangle =& \frac{12k_BT}{\pi^2 kf}\int_0^\infty \frac{dx}{x^2}\left\{1-\exp\left[-\frac{k\pi^2 t}{\zeta}x^2\right]\right\} \\ & \times\left\{\cos\left[\frac{\pi(n+1/2)p}{N+1}\right]+(f-1)\cos\left[\frac{\pi(N-n+1/2)(p-1/2)}{N+1/2}\right]\right\}\end{aligned} \tag{35}$$

The exponent in the integral will suppress the contribution for higher p-values. For a bead at the end of an arm, n equals N, the cosines can be taken to be 1 and the integral as the same as the integral for the central bead but with an extra factor f. For a bead in the middle of an arm, n equals $N/2$, in the long polymer limit the first cosine will be 1 for even values of p and 0 for odd values, and the second cosine will be $1/2$ for all values of p. This will give the same integral as for the bead at the end of an arm but smaller by a factor $1/2$. We thus find for the mean square displacement of a bead at the end of an arm

$$\langle \Delta \mathbf{R}_N^2(t)\rangle = \begin{cases} \dfrac{6k_BT}{\zeta}t, & \text{for } t<\dfrac{\zeta}{4k} \\ 12k_BT\sqrt{\dfrac{t}{\pi k\zeta}}, & \text{for } \dfrac{4\zeta}{\pi k}<t<\dfrac{N^2\zeta}{3k} \\ \dfrac{6k_BT}{\zeta fN}t, & \text{for } t>\dfrac{N^2\zeta}{3k}(3f-2)\end{cases}. \tag{36}$$

For the bead located exactly in the middle of an arm the mean square displacement becomes

$$\langle \Delta \mathbf{R}_{N/2}^2(t)\rangle = \begin{cases} \dfrac{6k_BT}{\zeta}t, & \text{for } t<\dfrac{\zeta}{4k} \\ 6k_BT\sqrt{\dfrac{t}{\pi k\zeta}}, & \text{for } \dfrac{4\zeta}{\pi k}<t<\dfrac{N^2\zeta}{3k} \\ \dfrac{6k_BT}{\zeta fN}t, & \text{for } t>\dfrac{N^2\zeta}{3k}(3f-2)\end{cases}. \tag{37}$$

Figure 2 shows the exact evaluation of Eq. (34) and demonstrates the validity of Eqs. (36-37). The behavior of a bead somewhere along the arm can also be extracted from these results. At first it will behave like the bead in the middle of an arm since locally they are the same. As time progresses it will either start feeling the end or the center of the polymer at first and mimic the behavior of the bead at the end or center respectively after which the mean square displacement will behave like that of the whole polymer.

4.4 Correlation function of a vector connecting a bead to the central bead

Consider the spatial vector connecting a bead in some arm to the central bead

$$\mathbf{r}_{i,n}(t) \equiv \mathbf{R}_{i,n}(t) - \mathbf{R}_0(t). \tag{38}$$

The correlation function $C_n(t) \equiv \langle \mathbf{r}_{i,n}(t)\cdot \mathbf{r}_{i,n}(0)\rangle$ is then given by

$$\begin{aligned}C_n(t) =& 16\sum_{p=1}^{N}\sin^2\left[\frac{\pi(n+1)p/2}{N+1}\right]\sin^2\left[\frac{\pi np/2}{N+1}\right]X_{pp}(t) \\ &+\frac{16}{f^2}\sum_{j,k,p=1}^{f,f,N}\cos^2\left[\frac{\pi(N-n+1/2)(p-1/2)}{N+1/2}\right]Y_{pp}^{(i,k)(i,j)}(t),\end{aligned} \tag{39}$$

where the cosines were reduced to sines for notational convenience. Having filled in the mode dynamics functions explicitly yields

$$\begin{aligned}C_n(t) =& \frac{24k_BT}{\zeta f(N+1)}\sum_{p=1}^{N}\sin^2\left[\frac{\pi(n+1)p/2}{N+1}\right]\sin^2\left[\frac{\pi np/2}{N+1}\right]\frac{1}{\alpha_{\mathbf{X}_p}}\exp\left[-\alpha_{\mathbf{X}_p}t\right] \\ &+\frac{12(f-1)k_BT}{\zeta f(2N+1)}\sum_{p=1}^{N}\cos^2\left[\frac{\pi(N-n+1/2)(p-1/2)}{N+1/2}\right]\frac{1}{\alpha_{\mathbf{Y}_p}}\exp\left[-\alpha_{\mathbf{Y}_p}t\right],\end{aligned} \tag{40}$$

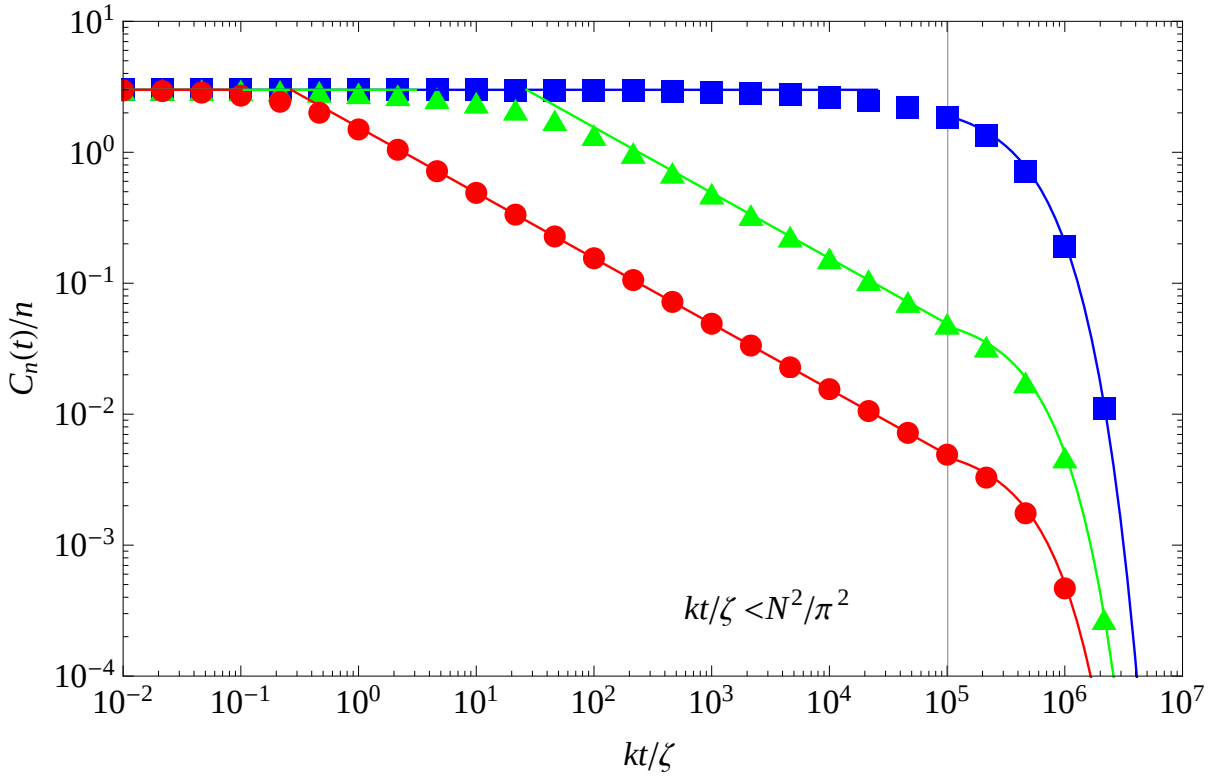

Figure 3: The scaled correlation function $C_n(t)/n$ as defined in Eqs. (38-39) in a double-logarithmic plot as a function of time. The correlation functions for several monomers in a symmetric star polymer as given by Eq. (40) were exactly evaluated with $f = 12$ arms of length $N = 10^3$ and other parameters put to 1. The red disks, green triangles, and blue squares correspond to $n = 1, 10$, and N for $C_n(t)$ respectively. Approximations for the correlation function in the short time scale $t < \zeta(n+1)^2/(4\pi^2 k)$, intermediate time scale $\zeta n^2(f-1)^2/(k\pi f^2) < t < N^2\zeta/(\pi^2 k)$, and the very long time scale $t > N^2\zeta/(\pi^2 k)$ as in Eq. (42) correspond solid lines. The approximation for intermediate times is only very accurate for small n, but for larger n this time domain becomes smaller or even non-existent as is the case for n equals N as can be seen in the figure.

where $\alpha_{\mathbf{X}_p}$ and $\alpha_{\mathbf{Y}_p}$ are defined in Eqs. (121-122). At very large and very small times the exact correlation functions for the modes in Eq. (24) can be used. At very small times the exponential can be omitted and the resulting equations solved using Eqs. (104b,104d). Adding the two terms then results in $C_n(t) = 3nk_BT/k$. To determine the region for which this approximation is valid we notice that the exponent is roughly 1 for $p^2 < \zeta N^2/(\pi^2 kt)$. The term in the summation will go to 0 for $p = 2(N+1)/(n+1)$ and so the largest contribution to the summation is for all the terms before this happens. Solving this for t where the large polymer limit is taken gives $t < \zeta(n+1)^2/(4\pi^2 k)$ for which the approximation is valid. For very large time values $t > (N^2\zeta)(\pi^2 k)$ only the lowest mode will give contribution. Since $f = 1, 2$ are two cases of linear chains we focus on $f \geq 3$ for which the second term in Eq. (40) will dominate. Taking the long polymer limit the sine can be expanded and the cosine reduced for notational convenience. For very large times the correlation function can thus be approximated by $C_n(t) = 12k_BTN/(\pi^2 k)\,(1 - \cos[\pi n/N])\exp\left[-\pi^2 kt/(4\zeta N^2)\right]$. For intermediate time values the second term can be approximated by a Gaussian integral in the long polymer limit by expanding the cosine for small n.

$$C_n(t) = \frac{6(f-1)n^2k_BT}{kf}\int_0^\infty dx \exp\left[-\frac{\pi^2 kt}{\zeta}x^2\right] = \frac{3(f-1)n^2k_BT}{kf\sqrt{\pi}}\left(\frac{kt}{\zeta}\right)^{-1/2}. \tag{41}$$

For $t > \zeta n^2 (f-1)^2/(\pi k f^2)$ the intermediate time approximation will be smaller and thus more accurate than the approximation for small times. Putting this together gives for $f \geq 3$

$$C_n(t) = \begin{cases} \dfrac{3nk_BT}{k}, & \text{for } t < \dfrac{\zeta(n+1)^2}{4\pi^2 k} \\ \dfrac{3(f-1)n^2 k_B T}{kf\sqrt{\pi}} \left(\dfrac{kt}{\zeta}\right)^{-1/2}, & \text{for } \dfrac{\zeta n^2 (f-1)^2}{k\pi f^2} < t < \dfrac{N^2\zeta}{\pi^2 k} \\ \dfrac{12k_BTN}{\pi^2 k}\left(1 - \cos\left[\dfrac{\pi n}{N}\right]\right) \exp\left[-\dfrac{\pi^2 k}{4\zeta N^2}t\right], & \text{for } t > \dfrac{N^2\zeta}{\pi^2 k} \end{cases} . \quad (42)$$

A graphical representation of the correlation function for a spatial vector between some monomer and the central monomer in a symmetric starpolymer with $f = 12$ and $N = 10^3$ is shown in Fig. 3.

5 Tadpole

A tadpole polymer can be seen as a star polymer where two of the three arms have the ends connected. Here we extend our calculations of the previous section and write down the exact solution for the eigenmodes for the specific case where the tadpole is built from a symmetric star polymer with arms of length N and a central bead with hydrodynamic radius three times as large as that of all the other beads. The Rouse modes are then a variation of the modes for a ring polymer combined with those for a star polymer. We use these eigenmodes to calculate the radius of gyration and mean square displacement of a monomer in the tadpole.

5.1 Eigenmodes

The first set of $N+1$ modes are like the $\mathbf{X}$ modes for the star polymer where all the arms behave the same. The second set of N modes are very similar to the $\mathbf{Y}$ modes of the star polymer where the ring takes on the role of an arm and the tail of the tadpole the role of another arm. The third set $\mathbf{Z}$ of N modes are Rouse modes for a ring polymer but specifically such that it is antisymmetric around the central bead. In Fig. 4 these three different modes are depicted for $p = 1$. We label the tadpole polymer

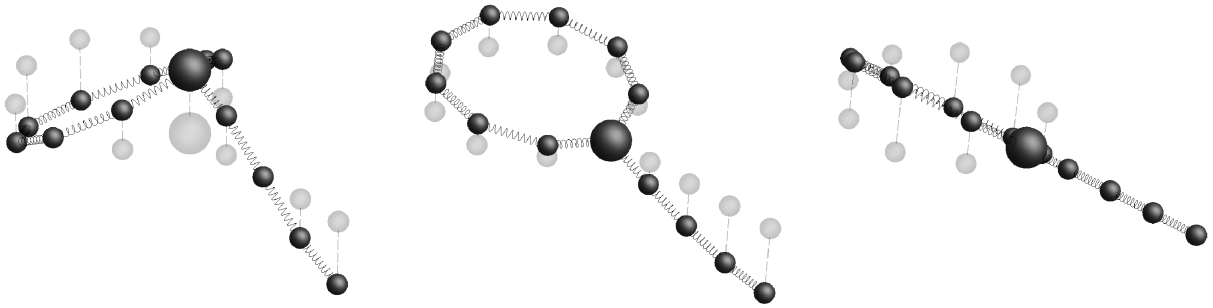

(a) (b) (c)

Figure 4: Three graphical representations of a tadpole polymer to visualize the Rouse modes. Depicted is a tadpole polymer, which can be seen as a symmetric star polymer with three arms consisting of four beads each where two arms are connected at the ends, with a central monomer which has a friction coefficient three times that of beads in the arms. The transparent configurations are polymers in the origin stretched in the xy-plane for visual convenience with no Rouse mode excited in the z-direction. The opaque configurations are like the transparent ones but with a pure $\mathbf{X}_1$ mode (a), $\mathbf{Y}_1$ mode (b), and $\mathbf{Z}_1$ mode (c) in the z-direction.

like a three-armed symmetric star polymer where arm one and two have the ends connected. The Rouse modes are then given by

$$\mathbf{X}_p(t) = \frac{1}{N+1}\left\{\cos\left[\frac{\pi p/2}{N+1}\right]\mathbf{R}_0(t) + \frac{1}{3}\sum_{a,n=1}^{3,N}\cos\left[\frac{\pi(n+1/2)p}{N+1}\right]\mathbf{R}_{a,n}(t)\right\}, \tag{43a}$$

$$\mathbf{Y}_q(t) = \frac{1}{4N+2}\sum_{n=1}^{N}\cos\left[\frac{\pi(N-n+1/2)(q-1/2)}{N+1/2}\right][\mathbf{R}_{1,n}(t) + \mathbf{R}_{2,n}(t) - 2\mathbf{R}_{3,n}(t)], \tag{43b}$$

$$\mathbf{Z}_q(t) = \frac{1}{2N+1}\sum_{n=1}^{N}\sin\left[\frac{\pi(N-n+1/2)q}{N+1/2}\right](\mathbf{R}_{1,n}(t) - \mathbf{R}_{2,n}(t)), \tag{43c}$$

with $p = 0 \ldots N$ and $q = 1 \ldots N$. The validity of these Rouse modes as the dynamical eigenmodes can be proved like for the star polymer in Appendix D. Let us define

$$\widetilde{\mathbf{X}}_n(t) = \mathbf{X}_0(t) + 2\sum_{p=1}^{N} \cos\left[\frac{\pi(n+1/2)p}{N+1}\right] \mathbf{X}_p(t), \tag{44a}$$

$$\widetilde{\mathbf{Y}}_n(t) = \frac{4}{3}\sum_{p=1}^{N} \cos\left[\frac{\pi(N-n+1/2)(p-1/2)}{N+1/2}\right] \mathbf{Y}_p(t), \tag{44b}$$

$$\widetilde{\mathbf{Z}}_n(t) = 2\sum_{p=1}^{N} \sin\left[\frac{\pi(N-n+1/2)p}{N+1/2}\right] \mathbf{Z}_p(t), \tag{44c}$$

so that the bead locations are given by

$$\mathbf{R}_0(t) = \widetilde{\mathbf{X}}_0(t) \tag{45a}$$

$$\mathbf{R}_{1,n}(t) = \widetilde{\mathbf{X}}_n(t) + \widetilde{\mathbf{Y}}_n(t) + \widetilde{\mathbf{Z}}_n(t), \tag{45b}$$

$$\mathbf{R}_{2,n}(t) = \widetilde{\mathbf{X}}_n(t) + \widetilde{\mathbf{Y}}_n(t) - \widetilde{\mathbf{Z}}_n(t), \tag{45c}$$

$$\mathbf{R}_{3,n}(t) = \widetilde{\mathbf{X}}_n(t) - 2\widetilde{\mathbf{Y}}_n(t). \tag{45d}$$

The dynamics for these modes are very similar as for the modes of the star polymer. The non-vanishing correlation functions for the modes of the tadpole are then given by

$$\langle [\mathbf{X}_0(t) - \mathbf{X}_0(0)]^2 \rangle = \frac{2k_BT}{\zeta(N+1)} t \tag{46a}$$

$$\langle \mathbf{X}_p(t) \cdot \mathbf{X}_q(0) \rangle = \frac{k_BT}{\zeta(N+1)} \frac{1}{2\alpha_{\mathbf{X}_p}} \exp\left[-\alpha_{\mathbf{X}_p} t\right] \delta_{pq} \tag{46b}$$

$$\langle \mathbf{Y}_p(t) \cdot \mathbf{Y}_q(0) \rangle = \frac{9k_BT}{4\zeta(2N+1)} \frac{1}{2\alpha_{\mathbf{Y}_p}} \exp\left[-\alpha_{\mathbf{Y}_p} t\right] \delta_{pq} \tag{46c}$$

$$\langle \mathbf{Z}_p(t) \cdot \mathbf{Z}_q(0) \rangle = \frac{3k_BT}{\zeta(2N+1)} \frac{1}{2\alpha_{\mathbf{Z}_p}} \exp\left[-\alpha_{\mathbf{Z}_p} t\right] \delta_{pq}, \tag{46d}$$

for $p, q = 1, \ldots N$ and

$$\alpha_{\mathbf{X}_p} = 4\frac{k}{\zeta}\sin^2\left[\frac{\pi p}{2N+2}\right], \alpha_{\mathbf{Y}_p} = 4\frac{k}{\zeta}\sin^2\left[\frac{\pi(p-1/2)}{2N+1}\right], \alpha_{\mathbf{Z}_p} = 4\frac{k}{\zeta}\sin^2\left[\frac{\pi p}{2N+1}\right]. \tag{47}$$

5.2 Radius of gyration

When the ends of two arms of a three armed symmetric star polymer are connected the mobility reduces and the radius of gyration will become smaller. Following the same steps as for the star polymer the radius of gyration is defined in the same way for the case when the central bead is three times as heavy as any other bead, and by plugging in the inverses it can be rewritten in terms of summations over the correlation functions of the modes at time zero. The radius of gyration squared for a long tadpole becomes:

$$R_g^2 = \frac{k_BTN}{k}\frac{5}{6}, \tag{48}$$

which is 5/7th of the radius of gyration of the same polymer but with the ends not connected.

5.3 Mean square displacement of a bead

Since the tadpole can be seen as a three armed star polymer with ends of two of the arms connected, the mean square displacement of the monomers in the third arm and that of the central monomer will not feel the effect of the connection of the two remaining arms. And so for the central monomer and the monomers in the tail of the tadpole the expressions will be exactly the same as in Eqs. (30,34) respectively. A monomer in the closed circle of the tadpole should behave in the same way as some monomer roughly in the middle of the tail:

$$\Delta\mathbf{R}_0(t) \equiv \mathbf{R}_0(t) - \mathbf{R}_0(0) \quad , \quad \Delta\mathbf{R}_{i,n}(t) \equiv \mathbf{R}_{i,n}(t) - \mathbf{R}_{i,n}(0). \tag{49}$$

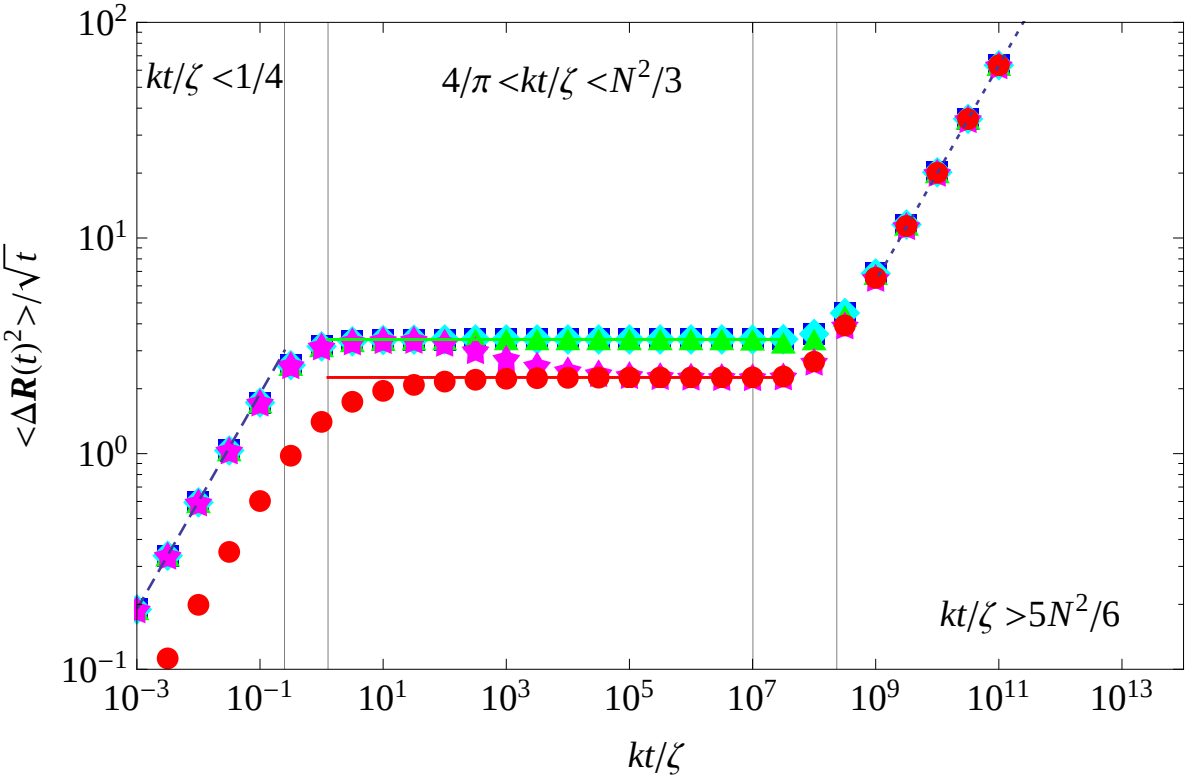

Figure 5: The scaled mean square displacement $\langle \Delta \mathbf{R}^2(t) \rangle / \sqrt{t}$ as a function of time. The mean square displacement of several beads in a tadpole made by a symmetric star polymer with ends of arm 1 and 2 connected as defined by Eq. (49) were exactly evaluated with $N = 10^4$ and other parameters put to 1. The red disks correspond to the mean square displacement of the central bead whereas the magenta stars, green triangles, cyan diamonds, and blue squares correspond to $i = 1$ and $n = 10^{-3}N, N/2, 9N/10,$ and N in Eq. (49) respectively. Unlike for the unconnected arms in the star polymer here there is no real difference between a monomer at the middle or end of the connected arm. A bead positioned somewhere along the arm will at first behave as if it were in the middle of the arm. If it is close enough to the heavy central bead the movement will be restricted and the mean square displacement will mimic that of the central bead. The short time scale $t < \zeta/(4k)$ and the very long time scale $t \gg 5N^2\zeta/(6k)$ for which $\langle \Delta \mathbf{R}^2(t) \rangle \sim t$ corresponding to the dashed and dotted lines are separated by a time during which $\langle \Delta \mathbf{R}^2(t) \rangle \sim \sqrt{t}$ corresponding to the solid lines as in agreement with Eqs. (50).

The mean square displacement for monomers in a tadpole can be described by

$$\langle \Delta \mathbf{R}_0^2(t) \rangle = \begin{cases} \dfrac{2k_BT}{\zeta}t, & \text{for } t < \dfrac{\zeta}{4k} \\ 4k_BT\sqrt{\dfrac{t}{\pi k\zeta}}, & \text{for } \dfrac{4\zeta}{\pi k} < t < \dfrac{N^2\zeta}{3k} \\ \dfrac{2k_BT}{\zeta N}t, & \text{for } t > \dfrac{N^2\zeta}{3k} \end{cases} , \tag{50a}$$

$$\langle \Delta \mathbf{R}_{3,N}^2(t) \rangle = \begin{cases} \dfrac{6k_BT}{\zeta}t, & \text{for } t < \dfrac{\zeta}{4k} \\ 12k_BT\sqrt{\dfrac{t}{\pi k\zeta}}, & \text{for } \dfrac{4\zeta}{\pi k} < t < \dfrac{N^2\zeta}{3k} \\ \dfrac{2k_BT}{\zeta N}t, & \text{for } t > \dfrac{7N^2\zeta}{3k} \end{cases} , \tag{50b}$$

$$\langle \Delta \mathbf{R}_{1,N}^2(t) \rangle = \langle \Delta \mathbf{R}_{3,N/2}^2(t) \rangle = \begin{cases} \dfrac{6k_BT}{\zeta}t, & \text{for } t < \dfrac{\zeta}{4k} \\ 6k_BT\sqrt{\dfrac{t}{\pi k\zeta}}, & \text{for } \dfrac{4\zeta}{\pi k} < t < \dfrac{N^2\zeta}{3k} \\ \dfrac{2k_BT}{\zeta N}t, & \text{for } t > \dfrac{5N^2\zeta}{6k} \end{cases} . \tag{50c}$$

Note that the domains of validity for the different behavior have changed in comparison to the star polymer. The exact sums for the monomers in a tadpole have a slightly different maximum as can be calculated using Eq. (104). Figure 5 shows the exact evaluation of Eq. (49) and demonstrates the validity of Eqs. (50).

6 Polymerized membrane

It is a natural question to ask if the analytical solution of the Rouse model can be generalized to higher dimensions, e.g., making it useful for the dynamics of polymerized membranes. There is a considerable amount interest in the properties of polymerized membranes [13]. The interest stems not only from the point of view of a fundamental understanding, but also because of their importance in biology and chemistry. Instances of polymerized membranes with a fixed connectivity can be found in 2D-cytoskeletons of cells [14, 15, 16] and graphite oxide sheets [17, 18, 19].

Static properties of polymerized membranes as a two-dimensional extension of (one-dimensional) linear polymers came into fashion in the late 80s. At that time the driving question centered on the equilibrium properties of polymerized membranes, in particular, the scaling of the radius of gyration of a polymerized membrane with its lateral size, while the corresponding scaling behavior for phantom and self-avoiding linear polymers were already well-known. Sophisticated renormalized group approaches were developed to this end [20, 21, 22, 23], accompanied by computer simulations [24, 25, 26, 27, 28, 29, 30, 31, 32]. A notable outcome of these studies is that the radius of gyration R_g of a membrane scales with its lateral size N as $R_g \sim \log N$ for phantom, and as $R_g \sim N$ for self-avoiding membranes.

In contrast to the equilibrium properties, the dynamical properties of membranes have been studied with less intensity. Apart from scaling analyses [33, 34, 35], the bulk of the research on the dynamics of polymerized membranes are heavily dominated by computer simulations [36, 37, 38, 39], leaving exact analytical results on the dynamics of membranes a relatively open area. In this paper we attempt to fill this void — we consider two-dimensional square-polymerized phantom membranes embedded in a three-dimensional space, both in the absence and the presence of tensile forces — and perform a Rouse mode analysis. We show that the Rouse modes are the *exact* eigenmodes of the membrane dynamics. Akin to the Rouse model for bead-spring linear polymers, our exercise allows us to exactly solve for the static and dynamic properties of phantom membranes; in this process also deriving the exact expression for the scaling of R_g as a function of the membrane's lateral size N (which confirms the $R_g \sim \log N$ scaling), as well as show increased fluctuations at the edge of the membrane [40, 41]. In particular, we draw the reader's attention to the exact solution under tensile forces, for which forces the membrane essentially encounters a flat geometry. Unlike a phantom membrane in equilibrium, in such a situation the membrane becomes essentially flat, does not get the opportunity to intersect itself, and therefore provides a highly useful and exactly soluble approach to the dynamics for a realistic model flat membrane. We also note that the methods are generalizable to arbitrary internal and spatial dimensions.

The structure of this section is as follows. We describe the dynamical equations without forces, and their diagonalization by the Rouse modes. Then we derive the scaling of the radius of gyration, the mean square displacement of a tagged bead and the autocorrelation function of a vector connecting two beads. After incorporating tensile forces in the dynamical equations we derive the new Rouse modes amplitude correlation functions. We also give the eigenmodes and their amplitude correlation functions for the n-torus which is a polymerized membrane with n internal dimensions all with periodic boundaries.

6.1 Eigenmodes

We consider a rectangular polymerized membrane, for which $N = L_1 \times L_2$ beads are connected in a perpendicular topology, with $\mathbf{R_n}(t)$ denoting the spacial position at time t of the bead internally labeled as $\mathbf{n}$. Naturally for a membrane it is convenient to take two numbers $\mathbf{n} = (n_1, n_2)$ for labeling the beads with $n_i = 1, \ldots, L_i$. The potential energy for a square-polymerized membrane is a simple extension of the Hamiltonian for a linear polymer in two internal dimensions

$$U = \frac{k}{2} \sum_{n_1,n_2=1}^{L_1-1,L_2} (\mathbf{R}_{n_1,n_2} - \mathbf{R}_{n_1+1,n_2})^2 + \frac{k}{2} \sum_{n_1,n_2=1}^{L_1,L_2-1} (\mathbf{R}_{n_1,n_2} - \mathbf{R}_{n_1,n_2+1})^2 \tag{51}$$

for some spring constant k.

In the absence of externally applied forces, in the overdamped limit the dynamics of each bead of the membrane is described by

$$\frac{d\mathbf{R_n}}{dt} = -\frac{1}{\zeta} \frac{\partial U}{\partial \mathbf{R_n}} + \mathbf{g_n}, \tag{52}$$

where ζ is the friction coefficient of the solvent and $\mathbf{g_n}$ is the thermal force on the $\mathbf{n}$-th bead. The

thermal forces are uncorrelated between different beads, as well as in time, i.e.,

$$\langle \mathbf{g_m}(t) \cdot \mathbf{g_n}(t') \rangle = \frac{6k_BT}{\zeta} \delta_{\mathbf{mn}} \delta(t - t'), \tag{53}$$

with Boltzmann constant k_B and temperature T.

For a linear polymer with positions $\mathbf{R}_n(t)$ of beads $n = 1, \ldots, N$ at time t the Rouse modes are given by [4, 5]

$$\mathbf{X}_p(t) = \frac{1}{N} \sum_{n=1}^{N} \cos\left[\frac{\pi(n - 1/2)p}{N}\right] \mathbf{R}_n(t), \tag{54}$$

with $p = 0, \ldots, N-1$ and the inverse given by

$$\mathbf{R}_n(t) = \mathbf{X}_0(t) + 2 \sum_{p=1}^{N-1} \cos\left[\frac{\pi(n - 1/2)p}{N}\right] \mathbf{X}_p(t) \tag{55}$$

The Rouse modes for the membrane are quite similar to those of the linear chain: since topologically the internal directions (connectivity) are orthogonal, the Rouse modes will be products of Rouse modes for a linear polymer. Below we introduce the following definitions for an elegant notation and proof of the independence of the Rouse modes.

First we define

$$\beta_{p_i} = \begin{cases} 2 & \text{if } p_i = 1, \ldots, L_i - 1 \\ 1 & \text{if } p_i = 0 \end{cases}, \quad \beta_{\mathbf{p}} = \beta_{p_1} \beta_{p_2} \tag{56}$$

and

$$f_{p_i}(n_i) = \cos\left[\frac{\pi p_i (n_i - 1/2)}{L_i}\right], \quad f_{\mathbf{p}}(\mathbf{n}) = f_{p_1}(n_1) f_{p_2}(n_2) \tag{57}$$

The orthogonality relation at the basis of the proof for the Rouse modes for a linear polymer chain in Eq. 102a can then be generalized for the membrane

$$\frac{1}{N} \sum_{\mathbf{n}} \beta_{\mathbf{p}} f_{\mathbf{p}}(\mathbf{n}) f_{\mathbf{q}}(\mathbf{n}) = \delta_{\mathbf{pq}}, \tag{58}$$

where the summation is taken over all allowed values of $\mathbf{n}$. The Rouse modes amplitudes and the corresponding inverse are then given by

$$\mathbf{X}_{\mathbf{p}}(t) = \frac{1}{N} \sum_{\mathbf{n}} f_{\mathbf{p}}(\mathbf{n}) \mathbf{R}_{\mathbf{n}}(t), \tag{59}$$

$$\mathbf{R}_{\mathbf{n}}(t) = \sum_{\mathbf{p}} \beta_{\mathbf{p}} f_{\mathbf{p}}(\mathbf{n}) \mathbf{X}_{\mathbf{p}}(t). \tag{60}$$

The position of the center-of-mass $\mathbf{R}_{\mathrm{cm}}(t)$ at time t simply equals $\mathbf{X_0}(t)$.

Next, we note that when the equations of motion from Eq. (52) for the beads are expressed one gets a term for each internal dimension equal to that of a term for a bead in a linear polymer. Taking the time derivative in Eq. (59) and plugging in the equations of motion for the beads and then the inverse we get

$$\frac{d\mathbf{X}_{\mathbf{p}}(t)}{dt} = -\alpha_{\mathbf{p}} \mathbf{X}_{\mathbf{p}}(t) + \mathbf{G}_{\mathbf{p}}(t) \tag{61}$$

$$\text{with } \alpha_{\mathbf{p}} \equiv 4\frac{k}{\zeta}\left(\sin^2\left[\frac{\pi p_1}{2L_1}\right] + \sin^2\left[\frac{\pi p_2}{2L_2}\right]\right) \text{ and } \mathbf{G}_{\mathbf{p}}(t) = \frac{1}{N} \sum_{\mathbf{n}} f_{\mathbf{p}}(\mathbf{n}) \mathbf{g}_{\mathbf{n}}(t), \tag{62}$$

i.e., the Rouse modes diagonalizes the equations of motion. This set of linearized differential equations can be solved just as for a linear polymer by using the correlation function for the thermal forces given by Eq. (53). By using the orthogonality relation in Eq. (58)

$$\langle \mathbf{G}_{\mathbf{p}}(t) \cdot \mathbf{G}_{\mathbf{q}}(t') \rangle = \frac{6k_BT}{\zeta N \beta_{\mathbf{p}}} \delta_{\mathbf{pq}} \delta(t - t'), \tag{63}$$

so that the following two-point correlation functions for the eigenmodes can be derived:

$$X_{\mathbf{00}}(t) \equiv \langle [\mathbf{X_0}(t) - \mathbf{X_0}(0)]^2 \rangle \equiv \langle [\mathbf{R}_{\rm cm}(t) - \mathbf{R}_{\rm cm}(0)]^2 \rangle = \frac{6k_BT}{\zeta N} t \tag{64}$$

$$X_{\mathbf{pq}}(t) \equiv \langle \mathbf{X_p}(t) \cdot \mathbf{X_q}(0) \rangle = \frac{3k_BT}{\zeta N \beta_{\mathbf{p}}} \frac{1}{\alpha_{\mathbf{p}}} \exp\left[-\alpha_{\mathbf{p}} t\right] \delta_{\mathbf{pq}} \quad \text{with } \mathbf{p} \neq \mathbf{0}. \tag{65}$$

Just like the case of a linear polymer, any correlation function of interest for the membrane can be derived using Eqs. (61-63). We address a few of them in the following subsections where, for the sake of simplicity, we restrict ourselves to square membranes with $L_1 = L_2 = L$, and thus $N = L \times L$.

6.2 Radius of gyration

The radius of gyration squared for the membrane is defined by

$$\begin{aligned} R_g^2 \equiv & \frac{1}{N} \sum_{\mathbf{n}} \left\langle [\mathbf{R_n}(t) - \mathbf{R}_{\rm cm}(t)]^2 \right\rangle \\ = & \frac{1}{N} \sum_{\mathbf{n}} \sum_{\mathbf{p}\neq\mathbf{0}} \sum_{\mathbf{q}\neq\mathbf{0}} \langle \mathbf{X_p}(t) \cdot \mathbf{X_q}(t) \rangle \beta_{\mathbf{p}} \beta_{\mathbf{q}} f_{\mathbf{p}}(\mathbf{n}) f_{\mathbf{q}}(\mathbf{n}), \end{aligned} \tag{66}$$

in which Eq. (60) is used for the second line. Having plugged in Eqs. (58) and (65) the squared radius

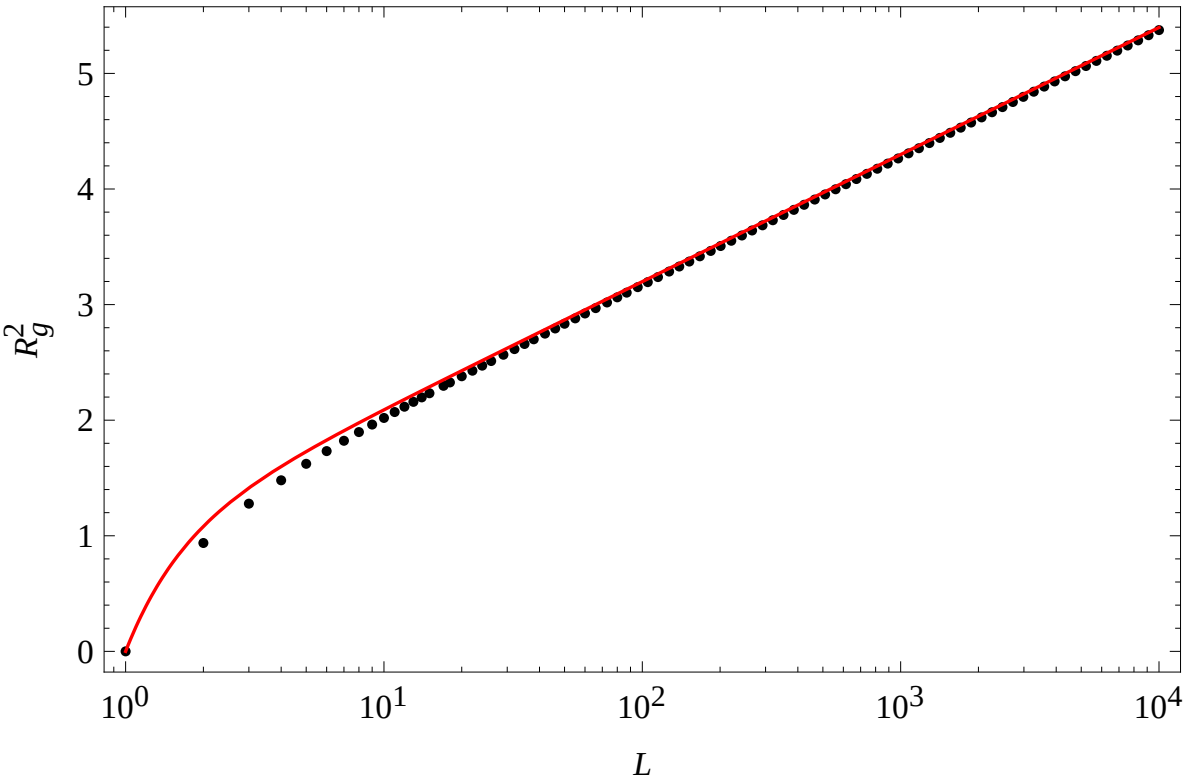

Figure 6: The radius of gyration squared R_g^2 for a square membrane as a function of $N = L \times L$ beads, with k_BT/k set to unity. The black dots represents the sum in Eq. (67) evaluated exactly for L up to $L = 10^4$, while the continuous red line represents the function $(N-1)/N + 3/(4\pi)\log N$.

of gyration reduces to

$$R_g^2 = \frac{3k_BT}{\zeta N} \sum_{\mathbf{p}\neq\mathbf{0}} \frac{1}{\alpha_{\mathbf{p}}}. \tag{67}$$

The summation (67), using the definition of $\alpha_{\mathbf{p}}$ (62), can be split into two parts:

$$R_g^2 = \frac{k_B T}{k}\left(\frac{3}{2N}\sum_{p=1}^{L-1}\sin^{-2}\left[\frac{\pi p}{2L}\right] + \frac{3k}{\zeta N}\sum_{p_1=1}^{L-1}\sum_{p_2=1}^{L-1}\frac{1}{\alpha_{\mathbf{p}}}\right) = \frac{k_B T}{k}\left(\mathcal{I}+\mathcal{J}\right). \tag{68}$$

The first term in Eq. (68) can be evaluated exactly: $\mathcal{I} = (N-1)/N$. For the second term we take the long polymer limit $N \gg 1$ so that $\alpha_{\mathbf{p}}$ can be expanded and the sum approximated by an integral with $x_i = p_i/L$ where the integral is over a unit square in the positive quadrant excluding the small area near the origin. The second approximation we make is replacing the area of integration by that of the positive quadrant of a unit circle excluding the small area near the origin which can be solved analytically

$$\mathcal{J} = \frac{3}{\pi^2}\int\frac{d\mathbf{x}}{x^2} = \frac{3}{2\pi}\int_{1/L}^{1}\frac{dr}{r} = \frac{3}{4\pi}\log N. \tag{69}$$

The radius of gyration squared for a square membrane in the long polymer limit thus becomes

$$R_g^2 = \frac{k_B T}{k}\left(\frac{N-1}{N} + \frac{3}{4\pi}\log N\right). \tag{70}$$

A comparison between the two terms in Eq. (70) shows that the second one is bigger than the first one for $N > 61$. In Fig. 6 we present a comparison between the analytical result (70) and the exact evaluation of Eq. (67) for L up to $L = 10^4$. Our result (70) confirms the $\log N$ scaling of R_g^2 obtained earlier by field-theory methods [20, 21, 22, 23].

6.3 Mean square displacement of a tagged bead

Let us define $\Delta\mathbf{R}_{\mathbf{n}}(t) \equiv \mathbf{R}_{\mathbf{n}}(t) - \mathbf{R}_{\mathbf{n}}(0)$ for the $\mathbf{n}$-th bead. We use Eq. (60) to write

$$\begin{aligned}\langle\Delta\mathbf{R}_{\mathbf{n}}(t)^2\rangle =& \langle[\mathbf{X}_{\mathbf{0}}(t) - \mathbf{X}_{\mathbf{0}}(0)]^2\rangle \\ &+ 2\sum_{\mathbf{p}\neq\mathbf{0}}\sum_{\mathbf{q}\neq\mathbf{0}}\beta_{\mathbf{p}}\beta_{\mathbf{q}}f_{\mathbf{p}}(\mathbf{n})f_{\mathbf{q}}(\mathbf{n})\left\{X_{\mathbf{pq}}(0) - X_{\mathbf{pq}}(t)\right\}.\end{aligned} \tag{71}$$

Using Eqs. (64-65) this simplifies to

$$\langle\Delta\mathbf{R}_{\mathbf{n}}(t)^2\rangle = \frac{6k_BT}{\zeta N}t + \frac{6k_BT}{\zeta N}\sum_{\mathbf{p}\neq\mathbf{0}}\frac{\beta_{\mathbf{p}}}{\alpha_{\mathbf{p}}}f_{\mathbf{p}}(\mathbf{n})^2\left\{1 - e^{-\alpha_{\mathbf{p}}t}\right\}. \tag{72}$$

At short times $kt/\zeta \ll 1/8$ the exponential in the second term can be expanded, and the sum is exactly evaluated. In comparison to the second term the first one can be neglected to obtain

$$\langle\Delta\mathbf{R}_{\mathbf{n}}(t)^2\rangle = \frac{6k_BT}{\zeta}t\frac{1}{N}\sum_{\mathbf{p}\neq\mathbf{0}}\beta_{\mathbf{p}}f_{\mathbf{p}}(\mathbf{n})^2 = \frac{6k_BT}{\zeta}t, \tag{73}$$

which agrees with the mean square displacement of a free bead, and confirms the wisdom that at short times the beads do not feel the connectivity.

At very long times the exponentials in Eq. (72) reduce to zero, the second term becomes a fixed number independent of t [but dependent on the location of the bead: the sum is largest when the bead is located at the corner of the membrane, and equals $6k_BT\left(\log N/\pi - \pi/4 + 2/3\right)/k$]; i.e., for $kt/\zeta \gg N\log N/\pi$ the first term of Eq. (71) dominates, and the motion of the tagged bead becomes simply diffusive, with the same diffusion coefficient as that of the center-of-mass.

At intermediate times the mean square displacement of the tagged bead will depend on its location on the membrane. We work out three difference cases when the tagged bead is (a) the central bead of the membrane, (b) located in the middle of an edge, and (c) a corner bead.

(a) For the mean square displacement of a bead at the center of the membrane $\langle\Delta\mathbf{R}_{\mathrm{m}}(t)^2\rangle$ the sum in Eq. (72) will only be over even values of p_i. In the long polymer limit the sum can be converted to an integral with $x_i = p_i/L$, such that

$$\langle\Delta\mathbf{R}_{\mathrm{m}}(t)^2\rangle = \frac{6k_BT}{\zeta}\int_0^1 dx_1\int_0^1 dx_2\frac{1}{\alpha_{\mathbf{p}}}\left\{1 - e^{-\alpha_{\mathbf{p}}t}\right\} = \frac{6k_BT}{\zeta}\int_0^t dt'\int_0^1 dx_1\int_0^1 dx_2 e^{-\alpha_{\mathbf{p}}t'}. \tag{74}$$

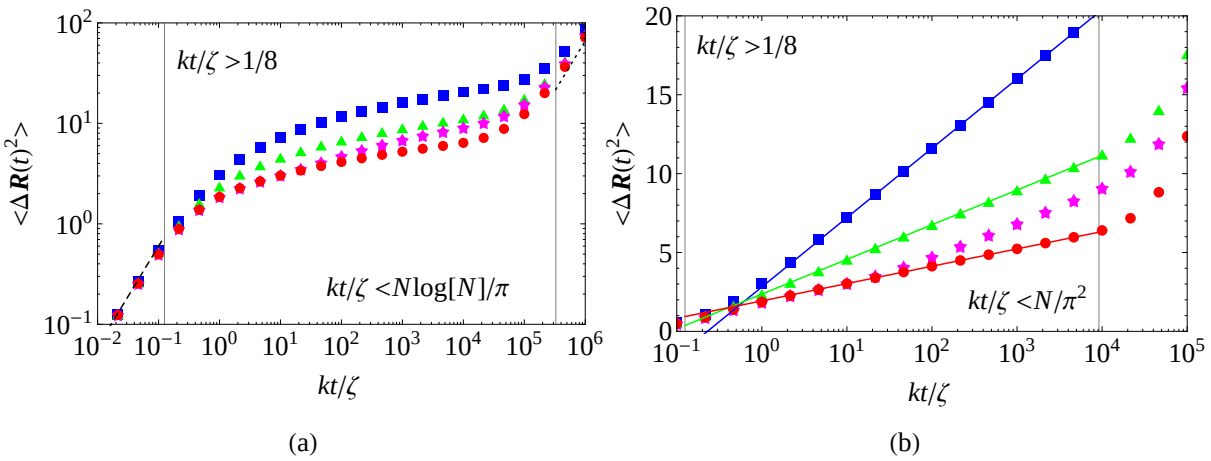

Figure 7: The mean square displacement $\langle \Delta \mathbf{R}_\mathbf{n}(t)^2 \rangle$ for beads in a square membrane as a function of scaled time kt/ζ. The sum in Eq. (72) was exactly evaluated for $k_B T/k = 1$ for beads at the center of the membrane, at the middle of an edge, and at a corner for $N = 301^2$ and the result is represented by the red disks, green triangles, and blue squares respectively. The magenta stars represent the exact evaluation for a bead with internal position $\mathbf{n} = (151, 5)$ to show the transition that the mean square displacement for a bead makes from one region to another. For very short times $kt/\zeta \ll 1/8$ the mean square displacement for all beads $\langle \Delta \mathbf{R}_\mathbf{n}(t)^2 \rangle \sim t$ thus behaving like that of a free bead as shown in Eq. (73) which is represented by the dashed line in (a). For very long times the mean square displacement for all beads $\langle \Delta \mathbf{R}_\mathbf{n}(t)^2 \rangle \sim t/N$ behaves like that of a mean square displacement of the center-of-mass which is represented by the dotted line in (a). In the intermediate time regime the mean square displacement for beads $\langle \Delta \mathbf{R}_\mathbf{n}(t)^2 \rangle \sim \log[kt/\zeta]$ as in agreement with Eqs. (76), (78), and (80), where the corresponding approximations are valid for $kt/\zeta \ll N/\pi^2$, and are represented by the red, green, and blue solid lines in (b) respectively.

We proceed with Eq. (74) by splitting the exponentials, resulting in two identical integrals which can be evaluated in terms of the modified Bessel function of the first kind $I_\alpha(z)$ and making a change of variables.

$$\langle \Delta \mathbf{R}_\mathrm{m}(t)^2 \rangle = \frac{6k_BT}{\zeta} \int_0^t dt' \left(\int_0^1 dx \exp\left\{ -\frac{4kt'}{\zeta} \sin^2\left[\frac{\pi}{2}x\right] \right\} \right)^2 = \frac{6k_BT}{k} \int_0^{\frac{kt}{\zeta}} dt' e^{-4t'} I_0^2(2t'). \tag{75}$$

To characterize the moderate time behavior of Eq. (75) we look at the asymptotic expansion $I_\alpha(z) = \exp(z)/\sqrt{2\pi z}$ and evaluated the integral so that

$$\langle \Delta \mathbf{R}_\mathrm{m}(t)^2 \rangle = \frac{3k_BT}{2\pi k} \left(\log\left[\frac{kt}{\zeta}\right] + C_\mathrm{m} \right), \tag{76}$$

where

$$C_\mathrm{m} = \lim_{x\to\infty} -\log[x] + 4\pi \int_0^x dt e^{-4t} I_0^2(2t) \approx 4.04. \tag{77}$$

(b-c) The same can be done for the mean square displacement for a bead located in the middle of an edge $\langle \Delta \mathbf{R}_\mathrm{e}(t)^2 \rangle$ and corner $\langle \Delta \mathbf{R}_\mathrm{c}(t)^2 \rangle$. The corresponding calculations are similar to those in (a), and they yield

$$\langle \Delta \mathbf{R}_\mathrm{e}(t)^2 \rangle = \frac{3k_BT}{\pi k} \left(\log\left[\frac{kt}{\zeta}\right] + C_\mathrm{e} \right), \tag{78}$$

where

$$C_\mathrm{e} = \lim_{x\to\infty} -\log[x] + 2\pi \int_0^x dt e^{-4t} \left(I_0(2t) + I_1(2t) \right) I_0(2t) \approx 2.47, \tag{79}$$

and

$$\langle \Delta \mathbf{R}_{\rm c}(t)^2 \rangle = \frac{6k_BT}{\pi k} \left(\log \left[\frac{kt}{\zeta} \right] + C_{\rm c} \right), \tag{80}$$

where

$$C_{\rm c} = \lim_{x\to\infty} -\log[x] + \pi \int_0^x dt e^{-4t} \left(I_0(2t) + I_1(2t) \right)^2 \approx 1.47. \tag{81}$$

Note that all constants C's can be evaluated up to arbitrary precision, and that the approximations (75), (77) and (79) are valid for $kt/\zeta \ll N/\pi^2$. In Fig. 7 we compare the exact evaluations from Eq. (72) and the corresponding approximations (73), (76), (78) and (80).

6.4 Autocorrelation function of a vector connecting two beads

In the most general case the vector $\mathbf{r_{mn}}(t) \equiv \mathbf{R_m}(t) - \mathbf{R_n}(t)$ connects two beads with internal coordinates $\mathbf{m}$ and $\mathbf{n}$ at time t. The autocorrelation function of this vector $D_{\mathbf{mn}}(t) \equiv \langle \mathbf{r_{mn}}(t) \cdot \mathbf{r_{mn}}(0) \rangle$ can be expressed in terms of the eigenmodes

$$D_{\mathbf{mn}}(t) = \frac{3k_BT}{\zeta N} \sum_{\mathbf{p}\neq\mathbf{0}} \frac{\beta_{\mathbf{p}}}{\alpha_{\mathbf{p}}} \left[f_{\mathbf{p}}(\mathbf{m}) - f_{\mathbf{p}}(\mathbf{n}) \right]^2 \exp\left[-\alpha_{\mathbf{p}} t \right]. \tag{82}$$

Like in the case for the mean square displacement of a tagged bead, the behavior of $D_{\mathbf{mn}}(t)$ depends on time and the internal positions of the beads, hence we only briefly outline the calculation procedure and state the results. We focus on two extreme cases (a) $D_{\rm c}(t)$ where the vector connecting the two beads located at the opposite corners of the membrane, and (b) $D_{\rm a}(t)$ where the vector connects two beads at position $\mathbf{n}$ and $\mathbf{n}+\mathbf{a}$ somewhere in the middle of the membrane for $a/L \equiv |\mathbf{a}|/L \ll 1$. We will generalize these results qualitatively for the cases when the locations of the beads and the distances between them are arbitrary.

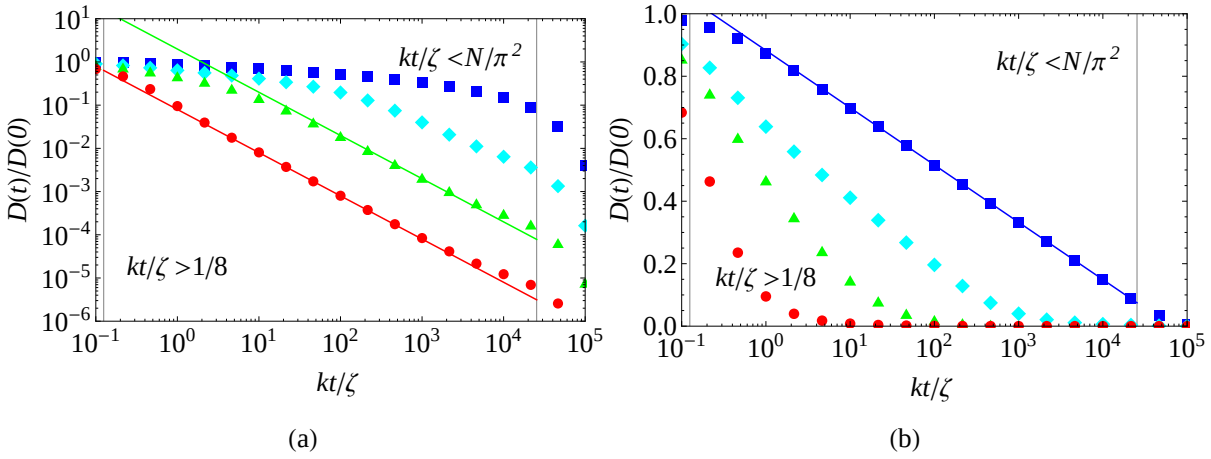

Figure 8: The scaled autocorrelation function $D_{\mathbf{mn}}(t)/D_{\mathbf{mn}}(0)$ of the vector connecting beads with internal position $\mathbf{m}$ and $\mathbf{n}$ in a square membrane as a function of scaled time kt/ζ. The sum in Eq. (82) was exactly evaluated with $k_BT/k = 1$ for two beads at positions [(251,251),(250,251)], [(251,254),(258,251)], [(1,1),(501,501)], and [(251,281),(281,251)] in the membrane with $N = 501^2$, with the results shown by the red disks, green triangles, blue squares, and cyan diamonds respectively. Note that the first two pairs of beads are very close to each other in the middle of the membrane where the third pair are two beads in opposing corners of the membrane; i.e., the first two cases correspond to $D_{\rm a}(t)/D_{\rm a}(0)$, while the third one corresponds to $D_{\rm c}(t)/D_{\rm c}(0)$. The function $D(t) \sim \log[kt/\zeta]$, as in agreement with Eq. (84) corresponding to the blue solid line in (b), for a duration that is larger when the beads are connected by a larger vector $\mathbf{a}$. For very small vectors $\mathbf{a}$ the behavior will shift to $D(t) \sim 1/t$ as derived in Eq. (83) corresponding to the red and green solid lines in (a) before $kt/\zeta \sim N/\pi^2$. The function $D(t)$ for the last pair shows a transition from logarithmic behavior to $D(t) \sim 1/t$ before the diffusive time regime.

Short times: For times $kt/\zeta \ll 1/8$ the exponent is roughly 1 and so the functions are constant. In case two beads are close neighbors the sum can be evaluated $D_{\rm a}(t) = k_BT(3/2+\log a)/k$, which is exact for $a = 1$, and a rough estimate $D_{\rm c}(t) = 6k_BT\log N/(\pi k)$ follows from a calculation similar to that performed for the radius of gyration.

Intermediate times: For $a/L \ll 1$ the sum for $D_{\rm a}(t)$ can be expanded in a and evaluated as

$$D_{\rm a}(t) = \frac{3\zeta k_BT}{8\pi k^2}\frac{a^2}{t}. \tag{83}$$

Further, it can be shown that the summation for $D_{\rm c}(t)$ equals that of $-\langle \Delta\mathbf{R}_{\rm c}(t)^2\rangle$ up to a constant, such that

$$D_{\rm c}(t) = D_{\rm c}(0) - \frac{6k_BT}{\pi k}\left(\log\left[\frac{kt}{\zeta}\right] + C_{\rm c}\right). \tag{84}$$

Long times: For $a/L \ll 1$ and $kt/\zeta \gg N/\pi^2$ only the lowest mode contributes to the summation and so expanding the correlation function in Eq. (82) yields

$$D_{\rm a}(t) = \frac{6k_BTa^2}{kN}\exp\left[-\frac{\pi^2 k}{\zeta N}t\right], \tag{85}$$

while

$$D_{\rm c}(t) = \frac{48k_BT}{\pi^2 k}\exp\left[-\frac{\pi^2 k}{\zeta N}t\right]. \tag{86}$$

It is interesting to note the differences in behavior for $D_{\rm a}(t)$ and $D_{\rm c}(t)$ at intermediate times. The reason behind this difference is as follows. For $D_{\rm a}(t)$ the beads are close and as a result they quickly become 'aware' of each other's presence. For $D_{\rm c}(t)$ on the other hand, the beads do not become 'aware' of each other's presence almost until $kt/\zeta \sim N/\pi^2$. Based on this observation we expect that when the beads are neither very close nor very far, there will be first a logarithmic decay (84) for $D_{\mathbf{mn}}(t)$, followed by a $1/t$ power-law decay (83) before the terminal exponential decay (85-86) sets in. The above results are verified by comparing the approximations to the exact evaluation of Eq. (82) for different pairs of beads in Fig. 8.

6.5 External tensile forces

Here we concentrate on presenting the exact eigenmodes when the membrane is stretched in two perpendicular directions by forces $\mathbf{F}_1$ and $\mathbf{F}_2$ applied at the edges of the membrane.

Adding tensile forces to the system ensures that each bead has its own mean position around which it fluctuates due to thermal forces. For large enough tensile forces the beads are far enough away from each other, and self-intersection of the membrane is avoided. Such a situation therefore mimics the behavior of a realistic flexible membrane under tension. The system is still exactly solvable by introducing the following term to the Hamiltonian

$$U_F = \sum_{n_1,n_2=1}^{L_1-1,L_2}\mathbf{F}_1\cdot(\mathbf{R}_{n_1,n_2}-\mathbf{R}_{n_1+1,n_2}) + \sum_{n_1,n_2=1}^{L_1,L_2-1}\mathbf{F}_2\cdot(\mathbf{R}_{n_1,n_2}-\mathbf{R}_{n_1,n_2+1}), \tag{87}$$

making the exercise of this section useful for practical purposes.

The mode amplitudes and their inverses are once again defined by Eqs. (59-60), but the following term $\mathbf{H_p}$ will be added to the right hand side of the differential equation in Eq. (61) in order to solve for the dynamics of the mode amplitudes:

$$\begin{aligned}\mathbf{H_p} &= \frac{1}{\zeta N}\sum_{\mathbf{n}} f_{\mathbf{p}}(\mathbf{n})\left[\mathbf{F}_1(\delta_{n_1L_1}-\delta_{n_11}) + \mathbf{F}_2(\delta_{n_2L_2}-\delta_{n_21})\right] \\ &= \frac{1}{\zeta}\left[\delta_{p_20}\{f_{p_1}(L_1)-f_{p_1}(1)\}\frac{\mathbf{F}_1}{L_1} + \delta_{p_10}\{f_{p_2}(L_2)-f_{p_2}(1)\}\frac{\mathbf{F}_2}{L_2}\right].\end{aligned} \tag{88}$$

Note that spatial symmetry for the modes is broken, and that Eq. (65) is replaced by similar equations but also depending on the spatial components i and j of the vectors.

$$X_{\mathbf{p}i\mathbf{q}j}(t) \equiv \langle \mathbf{X}_{\mathbf{p}i}(t)\mathbf{X}_{\mathbf{q}j}(0)\rangle = \frac{\mathbf{H}_{\mathbf{p}i}\mathbf{H}_{\mathbf{q}j}}{\alpha_{\mathbf{p}}^2} + \frac{k_BT}{\zeta N\beta_{\mathbf{p}}}\frac{1}{\alpha_{\mathbf{p}}}\exp\left[-\alpha_{\mathbf{p}}t\right]\delta_{\mathbf{pq}}\delta_{ij} \quad \text{with } \mathbf{p}\neq\mathbf{0}. \tag{89}$$

The assumption $\mathbf{F}_1 \perp \mathbf{F}_2$ is necessary in order for the modes to be the exact dynamical eigenmodes. If the tensile forces are not orthogonal, then it will result in correlations between some of the modes (and correspondingly a parallelogram-like structure of the membrane).

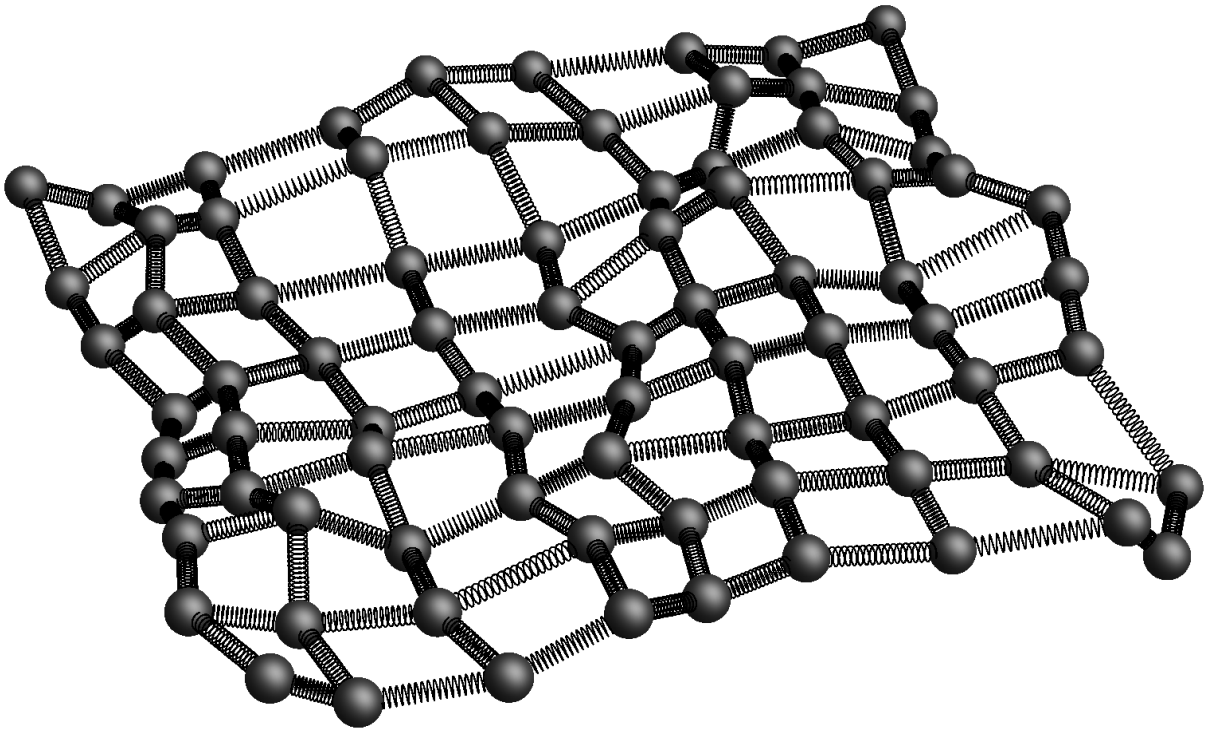

Figure 9: A randomly generated membrane consisting of 9×9 beads in a three dimensional space, with orthonormal tensile forces, $k_B T = 1/10$, and $k = \zeta = 1$. The black lines connects neighboring beads. Due to tensile forces the membrane gets a rectangular lattice like structure where thermal forces push the beads out of their mean positions.

It is of course interesting to investigate the transverse fluctuations of the membrane under lateral tension. Two observables we consider are the effective thickness and the additional surface area under thermal undulations. A quantity that can be used as a measure for the thickness of the membrane, is the standard deviation of the relative height of the bead in the middle of the membrane with respect to its mean position. In the limit of a continuous very large membrane, this thickness is given by

$$D \equiv \sqrt{\langle R_{\rm m}^2 \rangle} = \sqrt{\frac{k_B T}{4k}}. \tag{90}$$

We verified numerically that the fluctuations increase for beads near the edge of the membrane, in line with self-avoiding membranes [40, 41]. Note that this thickness is unaffected by the strength of the tensile forces.

A much more involved calculation is needed for the area of the membrane. Consider a very large square membrane with $N = L^2$ beads and perpendicular tensile forces $F_1 = F_2 = F$ of equal strength. We consider the case where the temperature is low enough, or the tensile forces are strong enough, such that the fluctuations of the beads around their equilibrium are small compared to the distances between two neighboring beads. The total area of the membrane can be written as the sum of areas of all triangles between the three beads with indices $(i, j), (i+1, j)$ and $(i, j+1)$ plus the sum of areas of all triangles with indices $(i+1, j), (i, j+1)$ and $(i+1, j+1)$; The expectation value for this area, in the continuum limit, is then given by

$$\langle A \rangle = \frac{F^2 (L-1)^2}{k^2} + \frac{k_B T (2L^2 - L)}{8k}. \tag{91}$$

The eigenmodes also give access to dynamical information. For instance, to obtain the mean vector connecting two neighboring beads in the membrane $\Delta \mathbf{R}_1(t) \equiv \mathbf{R}_{n_1+1,n_2}(t) - \mathbf{R}_{n_1,n_2}(t)$ with

$n_1 = 1, \ldots, L_1 - 1$ and $n_2 = 1, \ldots, L_2$, we use $\langle \mathbf{X}_\mathbf{p}(t) \rangle = \mathbf{H}_\mathbf{p}/\alpha_\mathbf{p}$, which can be proved by solving the differential equation in a similar fashion as for Eq. (89), such that

$$\langle \Delta \mathbf{R}_1(t) \rangle = \sum_\mathbf{p} \beta_\mathbf{p} \frac{\mathbf{H}_\mathbf{p}}{\alpha_\mathbf{p}} [f_\mathbf{p}(n_1 + 1, n_2) - f_\mathbf{p}(n_1, n_2)], \tag{92}$$

yielding $\Delta \mathbf{R}_1(t) = \mathbf{F}_1/k$ where Eq. (105) was used. The same is true for neighbors in the other internal direction so that for orthogonal tensile forces, on average, the membrane obtains is a flat rectangular structure. Further, the random thermal forces are gaussian distributed with a variation given by Eq. (1) such that $\langle \mathbf{X}^2_{\mathbf{p}i}(0) \rangle$ and $\langle \mathbf{X}_\mathbf{p}(0) \rangle$ can be used to derive the first two moments for every mode amplitude. We use these results to generate a random typical configuration for a membrane as shown in Figure 9.

6.6 n-Torus

The two dimensional polymerized membrane is a specific case of polymerized manifolds that can be solved by means of these eigenmodes. If the manifold has periodic boundaries in all internal directions, where the ring polymer is the one dimensional case, we consider the polymerized n-torus. The eigenmodes and notation are a little more elaborate in comparison to the two dimensional membrane in the previous section due to the arbitrary number of internal dimensions and the fact that in a ring there are two types of eigenmodes.

The n-torus polymer with $n \geq 1$ consists of N monomers chained together periodically in n directions. Let there be L_i monomers chained together in the i-th direction periodically so that $N = \prod_{i=1}^n L_i$ with $L_i \geq 3$ so that all monomers are identical and have $2n$ neighbors. We introduce parameters a_i,p_i,ϵ_i,$i \in \mathbb{N}^0$ with $i \in [1, n]$ and for convenience write in vector notation $\mathbf{a} = (a_1, a_2, \ldots, a_n)$ and the same for $\mathbf{p}$, $\boldsymbol{\epsilon}$ and $\mathbf{N}$. The position of a monomer is then given by $\mathbf{R}_\mathbf{a}(t)$ meaning that it is the a_1-th monomer in the first direction, the a_2-th monomer in the second direction up to the a_n-th monomer in the n-th direction so that $a_i \in [1, L_i]$. We also need a very important function $f^{\epsilon_i}_{p_i}(a_i)$ with $\epsilon_i \in [0, 1]$ defined as

$$f^{\epsilon_i}_{p_i}(a_i) = \begin{cases} \cos\left[\frac{2\pi p_i (a_i - 1/2)}{L_i}\right] & \text{if } \epsilon_i = 0 \\ \sin\left[\frac{2\pi p_i (a_i - 1/2)}{L_i}\right] & \text{if } \epsilon_i = 1 \end{cases}, \tag{93}$$

where

$$p_i \in \begin{cases} \left[0, \lfloor \frac{L_i - 1}{2} \rfloor\right] & \text{if } \epsilon_i = 0 \\ \left[1, \lceil \frac{L_i - 1}{2} \rceil\right] & \text{if } \epsilon_i = 1 \end{cases},$$

with $\lfloor x \rfloor$ and $\lceil x \rceil$, x rounded down and up to the nearest integer respectively. For short notation $f^\boldsymbol{\epsilon}_\mathbf{p}(\mathbf{a}) = \prod_{i=1}^n f^{\epsilon_i}_{p_i}(a_i)$.

We need an orthogonality relation similar to that in Eq. (102a) of the function $f^{\epsilon_i}_{p_i}(a_i)$ but for that we first need to define $\beta^{\epsilon_i}_{p_i}$ as

$$\beta^{\epsilon_i}_{p_i} = \begin{cases} 2 & \text{if } p_i \in \left[1, \lfloor \frac{L_i - 1}{2} \rfloor\right] \\ 1 & \text{if } (p_i, \epsilon_i) = (0, 0) \\ 1 & \text{if } L_i \text{ is even and } (p_i, \epsilon_i) = (\lceil \frac{L_i - 1}{2} \rceil, 1) \end{cases}, \tag{94}$$

where again for short notation write $\beta^\boldsymbol{\epsilon}_\mathbf{p} = \prod_{i=1}^n \beta^{\epsilon_i}_{p_i}$. The orthogonality relation then becomes

$$\frac{1}{N} \sum_\mathbf{a} \beta^\boldsymbol{\epsilon}_\mathbf{p} f^\boldsymbol{\epsilon}_\mathbf{p}(\mathbf{a}) f^\boldsymbol{\alpha}_\mathbf{q}(\mathbf{a}) = \delta_{\mathbf{pq}} \delta_{\boldsymbol{\epsilon}\boldsymbol{\alpha}}, \tag{95}$$

where δ is the Kronecker delta function and the sum is over all possible values of $\mathbf{a}$.

We define the modes $\mathbf{X}^\boldsymbol{\epsilon}_\mathbf{p}(t)$ and its inverse as

$$\mathbf{X}^\boldsymbol{\epsilon}_\mathbf{p}(t) = \frac{1}{N} \sum_\mathbf{a} f^\boldsymbol{\epsilon}_\mathbf{p}(\mathbf{a}) \mathbf{R}_\mathbf{a}(t), \tag{96}$$

$$\mathbf{R}_\mathbf{a}(t) = \sum_{\mathbf{p}, \boldsymbol{\epsilon}} \beta^\boldsymbol{\epsilon}_\mathbf{p} f^\boldsymbol{\epsilon}_\mathbf{p}(\mathbf{a}) \mathbf{X}^\boldsymbol{\epsilon}_\mathbf{p}(t), \tag{97}$$

which is easily verified by plugging Eq. (97) into Eq. (96) and using orthogonality relation Eq. (95) to simplify the expression. The mode $\mathbf{X}_{\mathbf{0}}^{\mathbf{0}}(t)$ can be physically interpreted as the center of mass at any given time t. In similar fashion as for the polymerized membrane we determined the equations of motion for the eigenmodes. They are given by

$$\frac{d\mathbf{X}_{\mathbf{p}}^{\boldsymbol{\epsilon}}(t)}{dt} = -\alpha_{\mathbf{p}}\mathbf{X}_{\mathbf{p}}^{\boldsymbol{\epsilon}}(t) + \mathbf{G}_{\mathbf{p}}^{\boldsymbol{\epsilon}}(t) \tag{98}$$

$$\text{with } \alpha_{\mathbf{p}} \equiv 4\frac{k}{\zeta}\sum_{i=1}^{n}\sin^2\left[\frac{\pi p_i}{L_i}\right] \text{ and } \mathbf{G}_{\mathbf{p}}^{\boldsymbol{\epsilon}}(t) = \frac{1}{N}\sum_{\mathbf{a}} f_{\mathbf{p}}^{\boldsymbol{\epsilon}}(\mathbf{a})\mathbf{g}_{\mathbf{a}}(t). \tag{99}$$

Now we plug in the correlation function for $\mathbf{g}_{\mathbf{a}}(t)$ and use the orthogonality relation Eq. (95) so that

$$\left\langle \mathbf{G}_{\mathbf{p}}^{\boldsymbol{\epsilon}}(t)\cdot\mathbf{G}_{\mathbf{q}}^{\boldsymbol{\alpha}}(t')\right\rangle = \frac{6D}{N\beta_{\mathbf{p}}^{\boldsymbol{\epsilon}}}\delta(t-t')\delta_{\mathbf{pq}}\delta_{\boldsymbol{\epsilon\alpha}}.$$

Finally we use this result in combination with the differential equation for the eigenmodes in Eq. (98) and its general solution found in Eq. (114) and Eq. (116) resulting in the expressions

$$X_{\mathbf{00}}(t) \equiv \langle[\mathbf{X}_{\mathbf{0}}(t)-\mathbf{X}_{\mathbf{0}}(0)]^2\rangle \equiv \langle[\mathbf{R}_{\mathrm{cm}}(t)-\mathbf{R}_{\mathrm{cm}}(0)]^2\rangle = \frac{6k_BT}{\zeta N}t, \tag{100}$$

$$X_{\mathbf{pq}}^{\boldsymbol{\epsilon\alpha}}(t) \equiv \langle\mathbf{X}_{\mathbf{p}}^{\boldsymbol{\epsilon}}(t)\cdot\mathbf{X}_{\mathbf{q}}^{\boldsymbol{\alpha}}(0)\rangle = \frac{3D}{N\beta_{\mathbf{p}}^{\boldsymbol{\epsilon}}}\frac{1}{\alpha_{\mathbf{p}}}\exp\left[-\alpha_{\mathbf{p}}t\right]\delta_{\mathbf{pq}}\delta_{\boldsymbol{\epsilon\alpha}} \quad \text{with } \mathbf{p},\boldsymbol{\epsilon}\neq\mathbf{0}. \tag{101}$$

7 Discussion

The Rouse model has proved to be a cornerstone for polymer dynamics. For bead-spring models of star and tadpole polymers with the topology of a symmetric star with f arms and tadpoles ($f = 3$, a special case), where the hydrodynamic radius of the central bead is f times as heavy as any other bead, we derived the exact expressions for the dynamical eigenmodes. We demonstrated the usefulness of this exercise by exact calculations of the radius of gyration, the mean square displacement of central bead and of various other individual beads, and the correlation function of an orientational vector. We repeat the exercise for polymers with a phantom manifold topology, in particular the membrane and n-torus. We have shown that a set of eigenmodes can be used to solve the membrane dynamics in the overdamped limit, and have demonstrated that many interesting properties can be analytically derived for the membrane using certain relations for these eigenmodes. Furthermore, we have shown that adding large enough tensile forces to the membrane system mimics the behavior of a realistic flexible membrane under tension: the eigenmodes can still be exactly solved analytically, making the analysis useful for practical purposes.

Although not explicitly stated here, these solutions for various bead-spring systems allow for solutions to certain other systems as well. In Sec. 4 we determined the eigenmodes for symmetric star polymers and in Sec. 5 showed that for a three-armed star polymer, if two of the arms are connected, the system is still solvable. This can also be generalized by letting $r < f/2$ pairs of arms be connected into r rings while not changing the other arms. In Sec. 6 we treated the two-dimensional manifold without periodic boundary conditions and the general manifold with periodic boundary conditions for every internal dimension. This could easily be generalized to a system with open or periodic boundaries per internal dimension resulting in for example the cylinder. Besides some very specific other types of polymers, like the comb polymer where all the beads in the middle have a specific friction coefficient, it seems like we discussed most systems that are similar to the linear polymer.

A Useful mathematical relations

The following relations are useful for calculating the Rouse modes

$$\frac{2}{N+1}\sum_{n=0}^{N}\cos\left[\frac{\pi(n+1/2)p}{N+1}\right]\cos\left[\frac{\pi(n+1/2)q}{N+1}\right]=\delta_{pq} \tag{102a}$$

$$\frac{4}{2N+1}\sum_{n=1}^{N}C_pC_q=\delta_{pq}\quad,\quad C_p=\cos\left[\frac{\pi(N-n+1/2)(p-1/2)}{N+1/2}\right], \tag{102b}$$

$$\frac{4}{2N+1}\sum_{n=1}^{N}C_pC_q=\delta_{pq}\quad,\quad C_p=\sin\left[\frac{\pi(N-n+1/2)p}{N+1/2}\right], \tag{102c}$$

for $p,q=1\ldots N$ and where the left hand side of Eq. (102a) equals $2\delta_{p0}$ for $p=0\ldots N$. A proof for the first orthogonality relation is given in Sec. B whereas the other relations can be proofed in similar ways or are assumed to be true after verifying numerically for a wide range of parameter values.

$$\sum_{p=1}^{N}\cos^2\left[\frac{\pi(n+1/2)p}{N+1}\right]=\frac{N}{2},\quad n=0\ldots N \tag{103a}$$

$$\sum_{p=1}^{N}\cos^2\left[\frac{\pi(N-n+1/2)(p-1/2)}{N+1/2}\right]=\frac{2N+1}{4},\quad n=1\ldots N \tag{103b}$$

$$\sum_{p=1}^{N}\sin^2\left[\frac{\pi(N-n+1/2)p}{N+1/2}\right]=\frac{2N+1}{4},\quad n=1\ldots N \tag{103c}$$

$$\sum_{p=1}^{N}\cos^2\left[\frac{\pi(n+1/2)p}{N+1}\right]\sin^{-2}\left[\frac{\pi p}{2N+2}\right]=\frac{N}{3}(2N+1)-2Nn+2n^2 \tag{104a}$$

$$\sum_{p=1}^{N}\cos^2\left[\frac{\pi(N-n+1/2)(p-1/2)}{N+1/2}\right]\sin^{-2}\left[\frac{\pi(p-1/2)}{2N+1}\right]=(2N+1)n \tag{104b}$$

$$\sum_{p=1}^{N}\sin^2\left[\frac{\pi(N-n+1/2)p}{N+1/2}\right]\sin^{-2}\left[\frac{\pi p}{2N+1}\right]=(2N+1-2n)n \tag{104c}$$

$$\sum_{p=1}^{N}\sin^2\left[\frac{\pi(n+1)p/2}{N+1}\right]\sin^2\left[\frac{\pi np/2}{N+1}\right]\sin^{-2}\left[\frac{\pi p/2}{N+1}\right]=\frac{n}{2}(N+1) \tag{104d}$$

The following relation holds for $a=1\ldots L-1$

$$\frac{2}{L}\sum_{p=1}^{L-1}\sin^-1\left[\frac{\pi p}{2L}\right]\sin\left[\frac{\pi ap}{L}\right]\cos\left[\frac{\pi p}{2L}\right]=1, \tag{105}$$

where the summation is over odd values of p and yields 0 for $a=L$.

$$\sum_{p=1}^{\infty}\frac{1}{p^2}=\frac{\pi^2}{6} \tag{106a}$$

$$\sum_{p=1}^{\infty}\frac{1}{(p-1/2)^2}=\frac{\pi^2}{2} \tag{106b}$$

B Orthogonality

The set of eigenmodes is a different but equivalent set of variables which diagonalizes the set of equations of motion. What follows here is a proof of an orthogonality relation that is at the basis of the eigenmodes.

$$M_{pq} = \frac{\beta_p}{N+1} \sum_{n=0}^{N} \cos\left[\frac{\pi(n+1/2)p}{N+1}\right] \cos\left[\frac{\pi(n+1/2)q}{N+1}\right] = \delta_{pq}, \tag{107}$$

where $\beta_0 = 1$ and $\beta_p = 2$ for $p = 1 \ldots N$. We start by expressing the trigonometric functions in terms of exponentials and so

$$M_{pq} = \frac{\beta_p}{4(N+1)} \sum_{n=0}^{N} r^{1/2} r^n + r^{-1/2} r^{-n} + s^{1/2} s^n + s^{-1/2} s^{-n}, \tag{108}$$

with $r = \exp\left[i\pi(p+q)/(N+1)\right]$ and $s = \exp\left[i\pi(p-q)/(N+1)\right]$. The solution to these geometric series are known and so the sum can be expressed as

$$M_{pq} = \frac{\beta_p}{4(N+1)} \left\{ \frac{r^{-(N+1)} - r^{N+1}}{r^{-1/2} - r^{1/2}} + \frac{s^{-(N+1)} - s^{N+1}}{s^{-1/2} - s^{1/2}} \right\}. \tag{109}$$

Replacing the exponentials by trigonometric functions again we get that

$$M_{pq} = \frac{\beta_p}{4(N+1)} \left\{ \frac{\sin\left[\pi(p+q)\right]}{\sin\left[\frac{\pi(p+q)}{2(N+1)}\right]} + \frac{\sin\left[\pi(p-q)\right]}{\sin\left[\frac{\pi(p-q)}{2(N+1)}\right]} \right\}. \tag{110}$$

Considering the domain of p, q the denominator of the first term will only go to zero if both p and q are zero, whereas the denominator of the second term will go to zero when p and q are equal. In all other cases the denominator is finite whereas the numerator will be zero for all integers p, q. Using L'Hôpital's rule in those specific cases we see that the terms become $2(N+1)$. Because of the factor β_p the sum will always be zero except when p and q are equal in which case it is one.

C Solving equations of motion for eigenmodes

The differential equation in Eq. (12) can not be exactly solved because the transform of the thermal forces $\mathbf{G}_p(t)$ is not exactly known for all times. We do however have the correlation functions in Eq. (13) and so the correlation functions for the amplitudes of the eigenmodes can be calculated.

The differential equations are of the form

$$\frac{dx(t)}{dt} = -\alpha x(t) + g(t), \tag{111}$$

which solved to $x(t)$ gives

$$x(t) = \int_{-\infty}^{t} dT e^{-\alpha(t-T)} g(T). \tag{112}$$

For the correlation function with positive t we get

$$\langle x(t)x(0)\rangle = \int_{-\infty}^{t} dT' \int_{-\infty}^{0} dT e^{-\alpha(t-T-T')} \langle g(T)g(T')\rangle \,, \tag{113}$$

where angular brackets represent the time average of the value. Assume $\langle g(T)g(T')\rangle = C\delta(T-T')$ so that:

$$\begin{aligned} \langle x(t)x(0)\rangle =& \int_{-\infty}^{t} dT' \int_{-\infty}^{0} dT e^{-\alpha(t-T-T')} C\delta(T-T') \\ =& Ce^{-\alpha t} \int_{-\infty}^{0} dT e^{2\alpha T} = \frac{C}{2\alpha} e^{-\alpha t}. \end{aligned} \tag{114}$$

In case α is zero the mode is diffusive and so we look at

$$x(t) - x(0) = \int_{0}^{t} dT g(T), \tag{115}$$

so that

$$\left\langle [x(t) - x(0)]^2 \right\rangle = \int_{0}^{t} dT' \int_{0}^{t} dT \, \langle g(T)g(T')\rangle = Ct. \tag{116}$$

D Determination of the Rouse modes of a star polymer

Several steps are needed to derive the dynamics of the modes in Eq. (24) from the equations of motion for a symmetric star polymer. It is useful to note that the modes are complete, which allows us to express the positions of the beads from the mode amplitudes, given by

$$\mathbf{R}_0 = \mathbf{X}_0 + 2\sum_{p=1}^{N} \cos\left[\frac{\pi p/2}{N+1}\right] \mathbf{X}_p \tag{117a}$$

$$\mathbf{R}_{i,n} = \mathbf{X}_0 + 2\sum_{p=1}^{N} \cos\left[\frac{\pi(n+1/2)p}{N+1}\right] \mathbf{X}_p + \frac{4}{f}\sum_{j,p=1}^{f,N} \cos\left[\frac{\pi(N-n+1/2)(p-1/2)}{N+1/2}\right] \mathbf{Y}_p^{(i,j)}. \tag{117b}$$

The correctness of these equations can be checked using the orthogonality relations from Eq. (102).

The dynamical equations of motion for the star polymer combined with the potential energy then result in the following equation of motion for the beads:

$$\frac{d\mathbf{R}_0}{dt} = -\frac{k}{\zeta}\left(\mathbf{R}_0 - \frac{1}{f}\sum_{i=1}^{f}\mathbf{R}_{i,1}\right) + \mathbf{g}_0 \tag{118a}$$

$$\frac{d\mathbf{R}_{i,1}}{dt} = -\frac{k}{\zeta}\left(2\mathbf{R}_{i,1} - \mathbf{R}_0 - \mathbf{R}_{i,2}\right) + \mathbf{g}_{i,1} \tag{118b}$$

$$\frac{d\mathbf{R}_{i,n}}{dt} = -\frac{k}{\zeta}\left(2\mathbf{R}_{i,n} - \mathbf{R}_{i,n-1} - \mathbf{R}_{i,n+1}\right) + \mathbf{g}_{i,n}. \tag{118c}$$

Note that $i = 1 \dots f$ and Eq. (118c) is valid for all $n = 2 \dots N$ where Eq. (117b) is needed to show that $\mathbf{R}_{i,N+1} = \mathbf{R}_{i,N}$. For convenience we define

$$\mathbf{R}_n = \frac{1}{f}\sum_{i=1}^{f}\mathbf{R}_{i,n} = \mathbf{X}_0 + 2\sum_{p=1}^{N}\cos\left[\frac{\pi(n+1/2)p}{N+1}\right]\mathbf{X}_p, \tag{119}$$

for $n = 0 \dots N$ which coincides with the inverse of $\mathbf{R}_0$ as given in Eq. (117a). Taking the time derivative on both sides of Eq. (22a), plugging in the equations of motion for the beads from Eq. (118), and using the definition above for which $\mathbf{R}_{-1} = \mathbf{R}_0$ and $\mathbf{R}_{N+1} = \mathbf{R}_N$ results in

$$\frac{d\mathbf{X}_p}{dt} = -\frac{1}{N+1}\frac{k}{\zeta}\sum_{n=0}^{N}\cos\left[\frac{\pi(n+1/2)p}{N+1}\right](2\mathbf{R}_n - \mathbf{R}_{n-1} - \mathbf{R}_{n+1}) + \mathbf{G}_p\ , \tag{120}$$

where $\mathbf{G}_p$ is the transform of the thermal forces which will be calculated later. By using Eq. (119), the trigonometric identities, namely the angle sum and difference identities and the power-reduction formula, and finally the orthogonality relation the set of differential equations becomes

$$\frac{d\mathbf{X}_p}{dt} = \begin{cases} -\alpha_{\mathbf{X}_p}\mathbf{X}_p + \mathbf{G}_p, & p = 1 \dots N \\ \mathbf{G}_0 \quad , & p = 0 \end{cases}, \quad \alpha_{\mathbf{X}_p} = 4\frac{k}{\zeta}\sin^2\left[\frac{\pi p}{2N+2}\right]. \tag{121}$$

The set of differential equations for the $\mathbf{Y}_p^{(i,j)}$ modes can be written down in a similar manner. We define $\mathbf{R}_n^{(i,j)} \equiv \mathbf{R}_{i,n} - \mathbf{R}_{j,n}$ and follow similar steps as for the $\mathbf{X}_p$ modes so that

$$\frac{d\mathbf{Y}_p^{(i,j)}}{dt} = -\alpha_{\mathbf{Y}_p}\mathbf{Y}_p + \mathbf{G}_p^{(i,j)}, \quad p = 1 \dots N, \quad \alpha_{\mathbf{Y}_p} \equiv 4\frac{k}{\zeta}\sin^2\left[\frac{\pi(p-1/2)}{2N+1}\right] \tag{122}$$

for some transform of the thermal forces $\mathbf{G}_p^{(i,j)}$.

With the above transformations, the set of differential equations for the beads have been transformed to a set of disconnected linear differential equations.

To find the relation for the modes as in Eq. (24) we must first determine the transform of the thermal forces $\mathbf{G}_p$ and $\mathbf{G}_p^{(i,j)}$. The transforms are equal to that of the modes in Eq. (22) but by replacing the position of the beads by their thermal force. Use that the thermal forces are uncorrelated in time and

between beads as in Eq. (1) and recall that the central bead has a friction coefficient f times as large as that of the other beads. The only nonvanishing functions with $p = 1 \dots N$ are

$$\langle \mathbf{G}_0(t) \cdot \mathbf{G}_0(t') \rangle = \frac{6k_BT}{\zeta f(N+1)} \delta(t-t') \tag{123a}$$

$$\langle \mathbf{G}_p(t) \cdot \mathbf{G}_q(t') \rangle = \frac{3k_BT}{\zeta f(N+1)} \delta_{pq} \delta(t-t') \tag{123b}$$

$$\left\langle \mathbf{G}_p^{(i,j)}(t) \cdot \mathbf{G}_q^{(k,l)}(t') \right\rangle = \frac{3k_BT}{\zeta(2N+1)} \delta_{pq} \delta(t-t') \frac{\delta_{(i,j)(k,l)}}{2}. \tag{123c}$$

With these, the set of differential equations can be solved exactly resulting in the following relations between modes:

$$\langle [\mathbf{X}_0(t) - \mathbf{X}_0(0)]^2 \rangle = \frac{6k_BT}{\zeta f(N+1)} t \tag{124a}$$

$$\langle \mathbf{X}_p(t) \cdot \mathbf{X}_q(0) \rangle = \frac{3k_BT}{\zeta f(N+1)} \frac{1}{2\alpha_{\mathbf{X}_p}} \exp\left[-\alpha_{\mathbf{X}_p} t\right] \delta_{pq} \tag{124b}$$

$$\langle \mathbf{Y}_p^{(i,j)}(t) \cdot \mathbf{Y}_q^{(k,l)}(0) \rangle = \frac{3k_BT}{\zeta(2N+1)} \frac{\delta_{(i,j)(k,l)}}{2} \frac{1}{2\alpha_{\mathbf{Y}_p}} \exp\left[-\alpha_{\mathbf{Y}_p} t\right] \delta_{pq}, \tag{124c}$$

where all other correlations between modes are strictly zero. By taking the long-polymer limit the sines can be expanded up to second order and the results are in Eq. (24).

References

[1] R. Keesman, G. T. Barkema, D. Panja, arXiv:1210.0774 **[cond-mat.soft]**.

[2] R. Keesman, G. T. Barkema, D. Panja, arXiv:1212.1024 **[cond-mat.soft]**.

[3] P. E. Rouse Jr., J. Chem. Phys. **21**, 1272 (1953)

[4] M. Doi, *Introduction to polymer physics,* Oxford University Press, Oxford, 1997.

[5] M. Doi and S. F. Edwards, *The theory of polymer dynamics*, Clarendon Press, Oxford (Reprinted, 2001).

[6] D. Panja, J. Stat. Mech. L02001 (2010).

[7] D. Panja, J. Stat. Mech. P06011 (2010).

[8] D. Panja and G.T. Barkema, J. Chem. Phys. **131**, 154903 (2009).

[9] G.T. Barkema, D. Panja and J.M.J. van Leeuwen, J. Chem. Phys. **134**, 154901 (2011).

[10] A. Ghosh, "Relaxation dynamics of branched polymers", Ph.D. thesis (Material Science and Engineering, Pennsylvania State University, 2007).

[11] H. Gao and K. Matyjaszewski, Prog. Polym. Sci. **34**, 317 (2009).

[12] D. Panja and G. T. Barkema, J. Chem. Phys. **131**, 154903 (2009).

[13] D. Nelson, T. Piran, and S. Weinberg, *Statistical Mechanics of Membranes and Surfaces*, World Scientific Publishing (Reprinted, 2004).

[14] R. Lipowsky and E. Sackmann, *Structure and Dymanics of Membranes, Handbook of Biological Physics Vol. 1*, Elsevier (1995).

[15] C. Picart and D. E. Discher, Biophys. J. **77**, 865 (1999).

[16] E. Sackmann, ChemPhysChem **3**, 237 (2002).

[17] T. Hwa, E. Kokufuta, and T. Tanaka, Phys. Rev. A **44**, R2235 (1991).

[18] M. S. Spector, E. Naranjo, S. Chiruvolu, and J. A. Zasadzinski, Phys. Rev. Lett. **73**, 2867 (1994).

[19] X. Wen et. al., Nature **355**, 426 (1992).

[20] Y. Kantor, M. Kardar, and D. R. Nelson, Phys. Rev. Lett. **57**, 791 (1986).

[21] Y. Kantor, M. Kardar, and D. R. Nelson, Phys. Rev. A **35**, 3056 (1987).

[22] K. Essafi, J.-P. Kownacki, and D. Mouhanna, Phys. Rev. Lett. **106**, 128102 (2011).

[23] J.-P. Kownacki and D. Mouhanna, Phys. Rev. E **79**, R040101 (2009).

[24] H. Koibuchi, N. Kusano, A. Nidaira, and K. Suzuki, Phys. Rev. E **69**, 066139 (2004).

[25] C. Münkel and D. W. Heermann, Phys. Rev. Lett. **75**, 1666 (1995).

[26] M. Plischke and D. Boal, Phys. Rev. A **38**, 4943 (1988).

[27] L. Radzihovsky and J. Toner, Phys. Rev. Lett. **75**, 4752 (1995).

[28] S. Mori and S. Komura, J. Phys. A: Math. Gen. **29**, 7439 (1996).

[29] D. Liu and M. Plischke, Phys. Rev. A **45**, 7139 (1992).

[30] F. F. Abraham, W. E. Rudge, and M. Plischke, Phys. Rev. Lett. **62**, 1757 (1989).

[31] D. M. Kroll and G. Gompper, J. Phys. I France **3**, 1131 (1993).

[32] Z. Zhang, H.T. Davis, and D. M. Kroll, Phys. Rev. E **48**, R651 (1993).

[33] M. Muthukumar, J. Chem. Phys. **88**, 2854 (1988).

[34] K. J. Wiese, Eur. Phys. J. B **1**, 269 (1998).

[35] K. J. Wiese, Eur. Phys. J. B **1**, 273 (1998).

[36] H. Popova and A. Milchev, Phys. Rev. E **77**, 041906 (2008).

[37] D. Boal, E. Levinson, D. Liu, and M. Plischke, Phys. Rev. A **40**, 3292 (1989).

[38] B. Y. Drovetsky, J. C. Chu, and C. H. Mak, J. Chem. Phys. **108**, 6554 (1998).

[39] S. B. Babu and H. Stark, Eur. Phys. J. E **34**, 136 (2011).

[40] G. Gompper and D. M. Kroll, J. Phys. I France **2**, 663 (1992).

[41] F. F. Abraham and D. R. Nelson, Science **249**, 393 (1990).